NATIONAL ADVISORY COMMITTEE FOR AERONAUTICS

TECHNICAL NOTE 3424

AERODYNAMIC CHARACTERISTICS OF SEVERAL

6-PERCENT-THICK AIRFOILS AT ANGLES OF ATTACK FROM

0° TO 20° AT HIGH SUBSONIC SPEEDS $M = 0.3 - 0.92$

By Bernard N. Daley and Douglas R. Lord

Langley Aeronautical Laboratory
Langley Field, Va.

NACA

Washington

May 1955

NATIONAL ADVISORY COMMITTEE FOR AERONAUTICS

TECHNICAL NOTE 3424

AERODYNAMIC CHARACTERISTICS OF SEVERAL

6-PERCENT-THICK AIRFOILS AT ANGLES OF ATTACK FROM

0° TO 20° AT HIGH SUBSONIC SPEEDS[1]

By Bernard N. Daley and Douglas R. Lord

SUMMARY

Two-dimensional tests of eight 6-percent-thick symmetrical airfoils of the supersonic and subsonic types were conducted in the Langley rectangular high-speed tunnel. Static pressures along the surfaces of each airfoil were measured over a Mach number range from 0.3 to the choking Mach number (about 0.92 at $\alpha = 0°$) at angles of attack from 0° to 20°. Total-pressure surveys in the wake were obtained for the same Mach number range at angles of attack from 0° to 8°. Schlieren photographs of the air flow were also obtained for representative conditions.

The aerodynamic characteristics of each of the airfoils have been determined from the measured pressure data. These results showed that the lift-curve slope of each of the airfoils decreased rapidly to a positive value approaching zero at angles of attack near 9° and roughly maintained this value up to the highest angle of attack tested.

When the maximum thickness was located at the 0.3-chord station rather than at the 0.7-chord station, the circular-arc and wedge-type airfoils produced higher lift-curve slopes and maximum lift coefficients, lower drag coefficients for a given lift coefficient, and improved pitching-moment characteristics. The variations with Mach number of the lift, drag, and pitching-moment coefficients are generally similar for the various types of airfoils tested. There appeared to be no factors which would prohibit the use of the sharp-leading-edge type of profiles at the subsonic speeds tested.

INTRODUCTION

The development of airfoil profiles having sharp leading edges, designed to minimize the wave resistance, has increased the feasibility of sustained flight of aircraft at supersonic speeds. Since any profile intended for supersonic flight must first traverse the subsonic speed

---

[1]Supersedes recently declassified NACA RM L9E19, 1949.

range, it is imperative that its force characteristics permit steady
and controllable flight throughout this range. Further, in many
applications the aerodynamic characteristics of the supersonic profiles
must permit subsonic maneuvering and landing.

The available results of previous investigations at subsonic Mach
numbers on 6-percent-thick airfoils having sharp leading edges are
limited to a high Reynolds number study of a circular-arc airfoil
section in the Langley two-dimensional low-turbulence tunnel (refer-
ence 1), an investigation of a double-wedge airfoil by the Ames
Laboratory (reference 2), and a low-angle-of-attack investigation of
seven of the models studied herein (reference 3). The purpose of this
investigation is to provide information on the force characteristics
of thin subsonic- and supersonic-type profiles at high angles of attack
by extending the tests of reference 3.

Eight 6-percent-thick symmetrical airfoils were tested at angles
of attack from $0°$ to $20°$. Test data were obtained by means of static-
pressure measurements along the surfaces of the airfoils and total-
pressure surveys in the wake.

SYMBOLS

M   stream Mach number

M_{ch} stream Mach number at choking

c_l section lift coefficient

$c_{m_c/4}$ section pitching-moment coefficient about quarter-chord
                location

c_d section drag coefficient

α angle of attack

$c_{l_{max}}'$ effective maximum section lift coefficient $\left(\text{lift coefficient}\right.$
                at $\dfrac{dc_l}{d\alpha} = 0.015\left.\right)$

P   pressure coefficient

APPARATUS AND TESTS

The tests were conducted in the Langley rectangular high-speed tunnel, which was a 4-inch by 18-inch closed-throat induction-type tunnel that draws air from the atmosphere.

Each airfoil was of 4-inch chord and completely spanned the test section along the 4-inch dimension. The models were supported by large circular end plates which were fitted into the tunnel walls in such a way as to rotate with the model and to retain continuity of the tunnel-wall surface. Between 36 and 40 static-pressure orifices were installed in the surfaces of each airfoil in two chordwise rows 1/4 inch from and on either side of the model center line. The number of orifices that could be installed depended on the shape of the model and its absolute thickness and, hence, was a minimum for the wedge-type airfoils. The two types of airfoils had the following profiles:

        Subsonic:
          NACA 0006-63   (reference 4)
          NACA 16-006   (reference 5)
          NACA 66-006   (reference 5)

        Supersonic (reference 3):   Designated herein:
          NACA 2S-(30)(03)-(30)(03)   C-3
          NACA 2S-(50)(03)-(50)(03)   C-5
          NACA 2S-(70)(03)-(70)(03)   C-7
          NACA 1S-(30)(03)-(30)(03)   W-3
          NACA 1S-(70)(03)-(70)(03)   W-7

In the supersonic-profile designation the letter C indicates the airfoil was of a circular-arc type, the letter W indicates the airfoil was of the wedge type, and the number following the letter indicates the location of maximum thickness in tenths of the chord from the leading edge. The profiles, with the static-pressure-orifice locations, are shown in figure 1.

Pressure-distribution measurements were made at angles of attack from $0°$ to $20°$ over a Mach number range from 0.30 to the choking Mach number (about 0.92 at $\alpha = 0°$ and 0.71 at $\alpha = 20°$). Wake surveys were made for the same Mach number range at angles of attack from $0°$ to $8°$. This Mach number range corresponded approximately to a Reynolds number range from 0.70 to 1.5×10^6. Schlieren photographs of the flow were also obtained for representative conditions. These photographs were taken with the knife edge perpendicular to the flow direction and with a spark of about 2-microsecond duration.

TUNNEL-WALL EFFECTS

The data obtained from this investigation have been corrected for the influence of the tunnel walls by the method of reference 6, which takes account of both solid and wake blockage. This correction is generally considered to be applicable to that Mach number range in which the influence of the choking condition on the flow is small. Static-pressure surveys along the wall showed that for all Mach numbers except those within 0.030 of the choking value there were no excessively large pressure gradients; accordingly, up to this point the data are believed to be quantitatively significant. This value of 0.030 is the same as that previously found in the low-angle-of-attack investigation of reference 3. The data within 0.030 of the choking Mach number are indicated in the figures in which they appear by dashed lines.

RESULTS

Representative aerodynamic data with corrected test points are presented in figure 2. The section-lift-coefficient data, obtained from the static-pressure distribution over the airfoils, are presented in figures 3 and 4. Near the leading edge, where it was impossible to install orifices on some of the profiles, the pressure distribution could not be defined exactly; and although special care was taken in fairing the pressure distribution in this region, the resultant aerodynamic characteristics are subject to some error. Variation of the effective maximum section lift coefficients with Mach number and profile parameters is given in figure 5. For the purpose of this analysis, the maximum lift coefficients were taken at the lowest angle of attack for which the slope of the lift-curve $\dfrac{dc_l}{d\alpha}$ became equal to 0.015. This criterion for the maximum lift, which is actually an effective maximum lift-coefficient, was used because of the failure of several of the lift-curves to attain zero slope for the angle-of-attack range of this investigation. The change in angle of attack for maximum lift coefficient with Mach number is shown in figure 6.

The section-drag-coefficient data are plotted against Mach number in figure 7 and against section lift coefficient in figure 8. For the angle-of-attack range from $0°$ to $8°$, the drag coefficients were computed by the wake-survey method of reference 7. Due to the extreme turbulence in the wake at angles of attack greater than $8°$, the drag coefficients at these higher angles were computed from the surface pressure distributions.

The data for section-pitching-moment coefficient about quarter-chord location are presented as functions of Mach number and section lift coefficient in figures 9 and 10, respectively. Moment coefficient is defined herein as the coefficient of the moment of the normal force about the quarter-chord location; this is essentially the true quarter-chord pitching-moment coefficient because the chordwise force had little effect on the pitching moment.

Representative pressure distributions and corresponding schlieren photographs are presented for the NACA 0006-63, C-3, and W-3 airfoils in figure 11.

DISCUSSION

Lift Coefficient

The variation of section lift coefficient with Mach number (fig. 3) is generally similar for both the subsonic- and supersonic-type airfoils. For angles of attack up to about 6°, the rate of change of lift coefficient with Mach number increased continuously to a maximum at $M \approx 0.8$; at higher Mach numbers the lift coefficient decreases rapidly. At angles of attack between 8° and 14°, the lift coefficient is erratic for Mach numbers less than about 0.55, then remains relatively constant until a Mach number of 0.70 is reached, after which the lift coefficient increases quite rapidly with Mach number to the limit of these tests. At higher angles of attack (16° to 20°) the curves are quite irregular; however, the lift coefficient tends to increase with Mach number.

At angles of attack up to about 6° (fig. 4), an increase in lift-curve slope $\frac{dc_l}{d\alpha}$ with increasing Mach number is observed. When the angle of attack reaches a value somewhere between 6° and 9°, the lift-curve slope decreased abruptly for all Mach numbers up to 0.75. For a Mach number of 0.80, the lift-curve slope in this angle-of-attack range tends to maintain a higher value than at the lower Mach numbers. Due to tunnel constriction effects, however, a Mach number of 0.80 could not be reached at higher angles of attack and this tendency could not be substantiated. Increasing the angle of attack beyond 9° gives a lift curve which is erratic both in magnitude and direction. Low-speed data for the C-5 airfoil from reference 1 are in good agreement with the data presented herein for this profile at $M = 0.40$. The general increase of lift with increasing angle of attack beyond the stall is contrary to the tendency of most thicker airfoils to stall with rapid loss in lift.

For the low angles of attack, the variation of lift-curve slope with Mach number is usually less for the supersonic-type than for the subsonic-type airfoils. The lift curves for the supersonic-type airfoils having a forward location of the maximum thickness have higher slopes than the airfoils with more rearward location of maximum thickness.

The data of figure 5(a) show that the maximum lifts of the three subsonic airfoils were not affected in any consistent manner by variation of maximum-thickness location, but decreasing the trailing-edge angle from 17° (NACA 16-006 airfoil) to 5° (NACA 66-006 airfoil) caused a consistent increase in effective maximum lift coefficient for the three airfoils. The absence of effect of maximum-thickness location on the maximum lift coefficient has been shown in low-speed tests of thin airfoils (reference 5), but the effect of change in trailing-edge angle at low speeds is not as well defined; for airfoils of 12-percent thickness (reference 8) no appreciable effect of trailing-edge angle was noticed, whereas for airfoils of lower thickness and sharp leading edges (reference 1) a decrease in trailing-edge angle increased the maximum lift coefficient.

The effective maximum lift coefficient for the supersonic-type airfoils (fig. 5(b)) generally increased with forward movement of the maximum-thickness location and with decrease in trailing-edge angle and tended to increase with leading-edge angle. The effect of leading-edge angle was more pronounced when the circular-arc and wedge-type airfoils were considered independently. The increase of effective maximum lift coefficient with decrease in trailing-edge angle for sharp-nose airfoils is in agreement with the results of low-speed tests on 6- and 10-percent-thick circular-arc airfoils (reference 1). (The leading-edge angles, trailing-edge angles, and maximum-thickness locations presented herein are interrelated. Leading- and trailing-edge angles were determined from tangents at the 0- and 100-percent-chord stations.)

At Mach numbers up to about 0.65 there is little variation of effective maximum lift coefficient with Mach number (fig. 5(a)) for all airfoils except the wedge type. Beyond a Mach number of 0.65 the maximum lifts of most of the airfoils increase in a manner similar to that previously observed in references 2 and 9. The angle of attack for maximum lift coefficient (fig. 6) shows a general decrease with increasing Mach number for all of the airfoil sections.

In general, it appears that for the subsonic-type airfoil sections tested in this investigation the best lift characteristics - that is, lift-curve slope and maximum section lift coefficient - were exhibited by the NACA 66-006 airfoil. For the supersonic-type sections, the best lift characteristics were obtained with the airfoils having their

maximum-thickness location at the most forward position tested. The general lift characteristics are similar for all of the profiles, and none of the supersonic-type profiles show peculiar lift characteristics which would prohibit their use in the subsonic speed range covered by these tests.

Drag Coefficient

The effects of compressibility on the section drag coefficients are shown by figure 7 to be generally the same for all of the airfoils tested and similar to previous test results for thin symmetrical airfoils at low angles. At angles of attack from 10° to 20° the curves are quite erratic throughout the Mach number range.

In figure 8 differences in drag coefficient of the order of 0.005 are evident for the various airfoils at very low lift coefficients (previously shown in reference 3). The subsonic-type airfoils generally had the lowest drag coefficient and the wedge-type airfoils had the highest drag coefficient. At higher lift coefficients a general decrease in drag coefficient for a given lift coefficient occurs with forward movement of maximum-thickness location as a result of the improved lift characteristics previously discussed for those supersonic airfoils having their maximum-thickness location forward. A very rapid rise in drag coefficient occurs after the lift coefficient reaches a value near $c_{l_{max}}'$ (about 0.6 to 0.7), the rise generally occurring at a higher lift coefficient for the subsonic-type than for the supersonic-type airfoils.

Increases in Mach number (within the range presented) have little effect on the data at very low lift coefficients but generally result in increases in lift-drag ratio at all lift coefficients below the stall. This effect of Mach number on lift-drag ratio is most pronounced for the NACA 16-006 and NACA 66-006 airfoils. The rapid increase in drag coefficient near maximum lift observed at all Mach numbers up to 0.70 is reduced considerably at a Mach number of 0.80.

Although the drag coefficients of the supersonic-type airfoils are generally higher than those of the subsonic airfoils, the differences in drag coefficient are not so large that the use of the sharp-nose profiles would excessively affect the performance of supersonic aircraft within the subsonic speed range investigated.

Quarter-Chord Pitching-Moment Coefficient

The variation of the section quarter-chord pitching-moment coefficient $c_{m_c/4}$ with stream Mach number (fig. 9) may best be discussed by considering two angle-of-attack ranges, one from $2°$ to $10°$ and the other from $12°$ to $20°$. In the low angle-of-attack range, the variation of moment coefficient with Mach number (at constant angle of attack) is small and regular until a Mach number of 0.70 or greater is reached. With further increase in Mach number, the moment coefficient increases negatively quite rapidly. For the higher angles, the moment curves are erratic throughout the Mach number range. The sharp increase in negative slope is not present at the highest Mach numbers; however, there is a general negative trend throughout the Mach number range. The effect of Mach number on the variation of $c_{m_c/4}$ with c_l for these airfoils can best be seen in figure 10. For the subsonic-type airfoils, the effect of Mach number on pitching-moment coefficient is smallest for the NACA 0006-63 airfoil. The supersonic-type airfoils all show similar effects of Mach number on pitching-moment-coefficient behavior with the exception of the C-7 airfoil, which is definitely inferior.

The effect of increasing lift coefficient on pitching-moment coefficient can be shown by the moment polars of figure 10. Good agreement was found between the moment data for the C-5 profile of reference 1 and the $M = 0.40$ data presented in figure 10(e). At low lift coefficients the two supersonic-type airfoils having their maximum thickness at the 70-percent-chord station produced higher rates of change of moment coefficient with lift coefficient than did those airfoils whose maximum-thickness locations were ahead of or at the 50-percent-chord station. For lift coefficients near $c_{l_{max}}'$ (about 0.6), a rapid rise in negative pitching-moment coefficient occurs for all of the airfoils. There is some indication that at a Mach number of 0.80 this sudden change in slope is diminished. For the subsonic-type profiles, the NACA 0006-63 seemed to give the most steady variation of pitching-moment coefficient with lift coefficient. For the supersonic-type sections, those airfoils having a forward location of the maximum thickness had smaller values of $\dfrac{dc_{m_c/4}}{dc_l}$ in the lower angle-of-attack range and smoother variations of moment with lift. Although those sharp-nose airfoils having their maximum thickness at the 70-percent-chord station exhibit undesirable moment characteristics, it appears that the supersonic-type profiles with the more forward locations of maximum thickness would be generally as acceptable as the subsonic-type profile for practical applications within the speed range of these tests.

Schlieren Photographs and Pressure Distributions

The schlieren photographs and pressure-distribution diagrams shown in figure 11 are representative of flow conditions over the airfoils investigated. The leading-edge attached-shock phenomenon, first reported in reference 3, is shown to occur at angles of attack as high as 8° and was observed at an angle of attack of 12° at the choking Mach number (not presented). At higher angles of attack only separation was observed, but the maximum attainable Mach number was reduced with increase in angle of attack. The pressure-distribution diagrams show that at high angles of attack this separation has eliminated the effect of change in upper-surface contour. These diagrams also show that the loading near the trailing edge is very high at angles of attack of 8° or greater.

CONCLUSIONS

Two-dimensional tests of 6-percent-thick symmetrical airfoils of various circular-arc, wedge, and rounded leading-edge profiles at high subsonic Mach numbers indicate the following conclusions:

1. At angles of attack near 9° the lift-curve slope of each of the airfoils decreased rapidly to a positive value approaching zero and roughly maintained this value up to the highest angle of attack tested.

2. When the maximum thickness was located at the 0.3-chord station rather than at the 0.7-chord station, the circular-arc and wedge-type airfoils produced higher lift-curve slopes and maximum lift coefficients, lower drag coefficients for a given lift coefficient, and improved pitching-moment characteristics.

3. The variations with Mach number of the lift, drag, and pitching-moment coefficients are generally similar for the various type airfoils tested. There appeared to be no factors which would prohibit the use of the sharp-leading-edge-type profiles at the subsonic speeds tested.

Langley Aeronautical Laboratory,
National Advisory Committee for Aeronautics,
Langley Field, Va., May 3, 1949.

REFERENCES

1. Cahill, Jones F., Underwood, William J., Nuber, Robert J., and
   Cheesman, Gail A.: Aerodynamic Forces and Loadings on Symmetrical
   Circular-Arc Airfoils With Plain Leading-Edge and Plain Trailing-
   Edge Flaps. NACA Rep. 1146, 1953. (Supersedes NACA RM L6K22 by
   Underwood and Nuber, NACA RM L7H04 by Underwood and Nuber, NACA
   RM L50H17a by Nuber and Cahill, and NACA RM L9G20 by Nuber and
   Cheesman.)

2. Solomon, Joseph, and Henney, Floyd W.: The Subsonic Aerodynamic
   Characteristics of Two Double-Wedge Airfoil Sections Suitable
   for Supersonic Flight. NACA RM A6G24, 1947.

3. Lindsey, W. F., Daley, Bernard N., and Humphreys, Milton D.: The
   Flow and Force Characteristics of Supersonic Airfoils at High
   Subsonic Speeds. NACA TN 1211, 1947.

4. Stack, John, and Von Doenhoff, Albert E.: Tests of 16 Related Air-
   foils at High Speeds. NACA Rep. 492, 1934.

5. Abbott, Ira H., Von Doenhoff, Albert E., and Stivers, Louis S., Jr.:
   Summary of Airfoil Data. NACA Rep. 824, 1945. (Supersedes NACA
   WR L-560.)

6. Allen, H. Julian, and Vincenti, Walter G.: Wall Interference in a
   Two-Dimensional-Flow Wind Tunnel, With Consideration of the Effect
   of Compressibility. NACA Rep. 782, 1944. (Supersedes NACA WR A-63.)

7. Baals, Donald D., and Mourhess, Mary J.: Numerical Evaluation of the
   Wake-Survey Equations for Subsonic Flow Including the Effect of
   Energy Addition. NACA WR L-5, 1945. (Formerly NACA ARR L5H27.)

8. Loftin, Laurence K., Jr.: Theoretical and Experimental Data for a
   Number of NACA 6A-Series Airfoil Sections. NACA Rep. 903, 1948.
   (Supersedes NACA TN 1368.)

9. Cleary, Harold, E.: Effects of Compressibility on Maximum Lift Coef-
   ficients for Six Propeller Airfoils. NACA WR L-514, 1945. (For-
   merly NACA ACR L4L21a.)

NACA 0006-63

NACA 16-006

NACA 66-006

C-3

Orifice locations

C-5

C-7

W-3

W-7
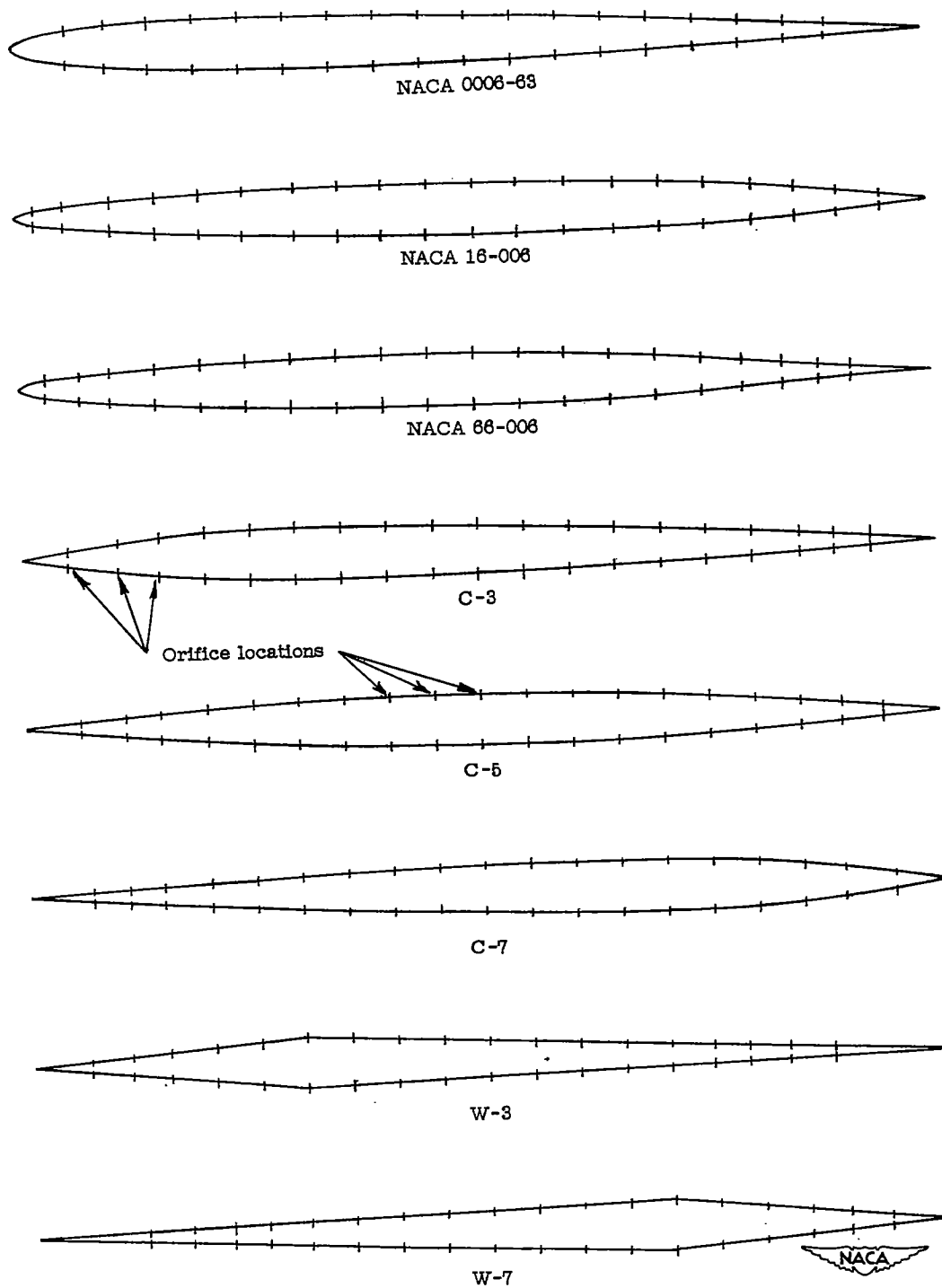
NACA

Figure 1.— Airfoil profiles and static-pressure-orifice locations.
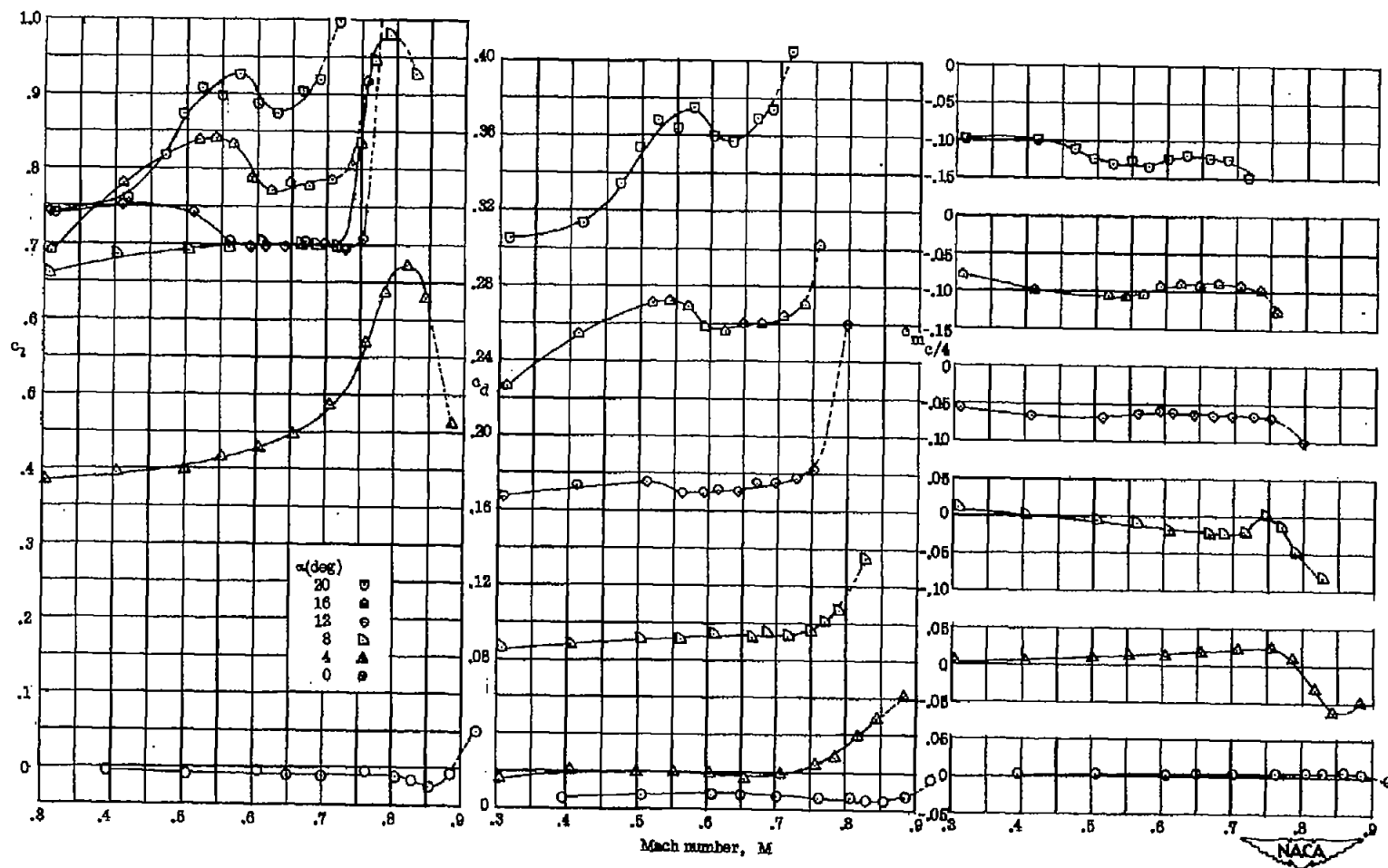
Figure 2.- Representative variations with Mach number of the force characteristics of the NACA 16-006 airfoil. (Curves are dashed for data from $(M_{ch} - 0.030)$ to $M_{ch}.$)
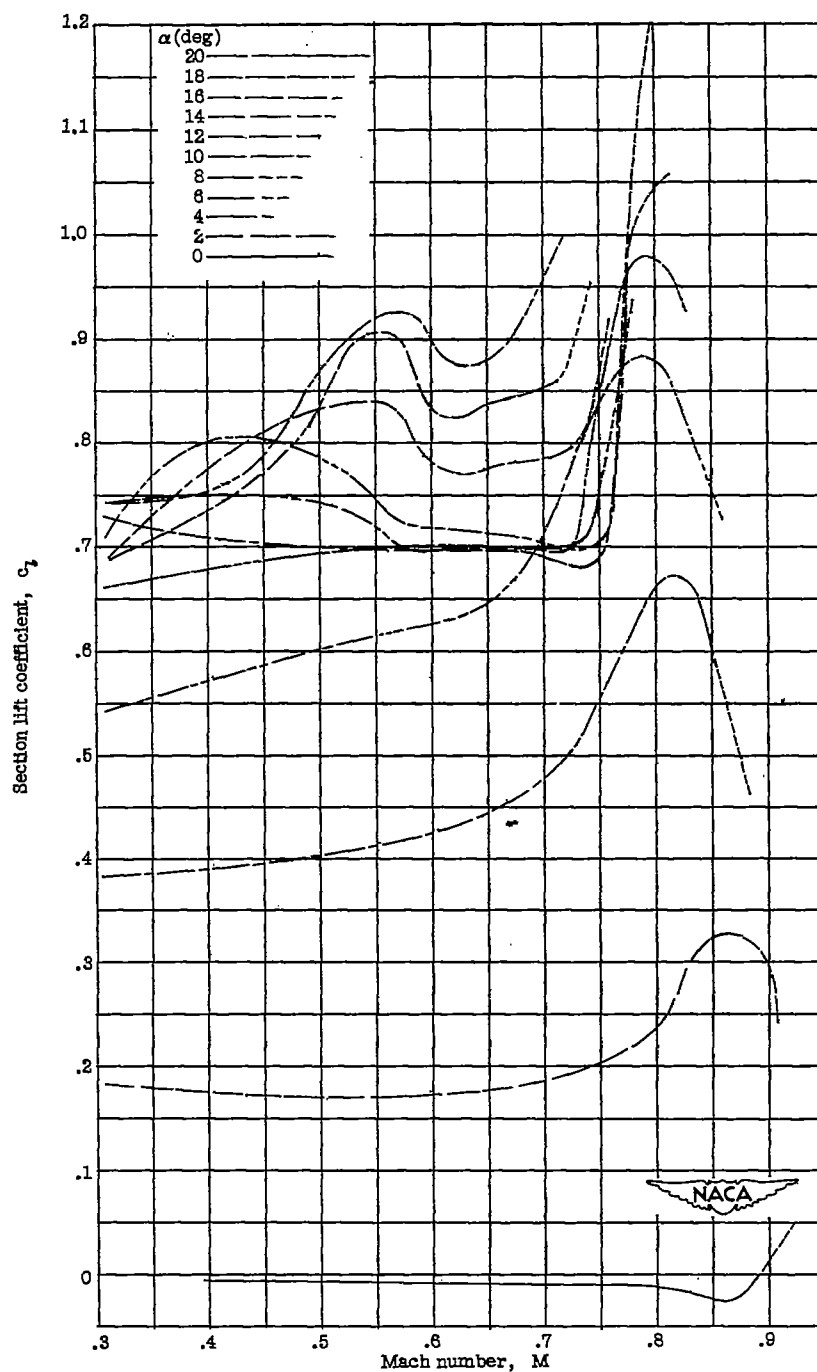
(a) NACA 16-006 airfoil.

Figure 3.- Variation of section lift coefficient c_l with Mach number M. (Curves are dashed for data from $(M_{ch} - 0.030)$ to M_{ch}.)
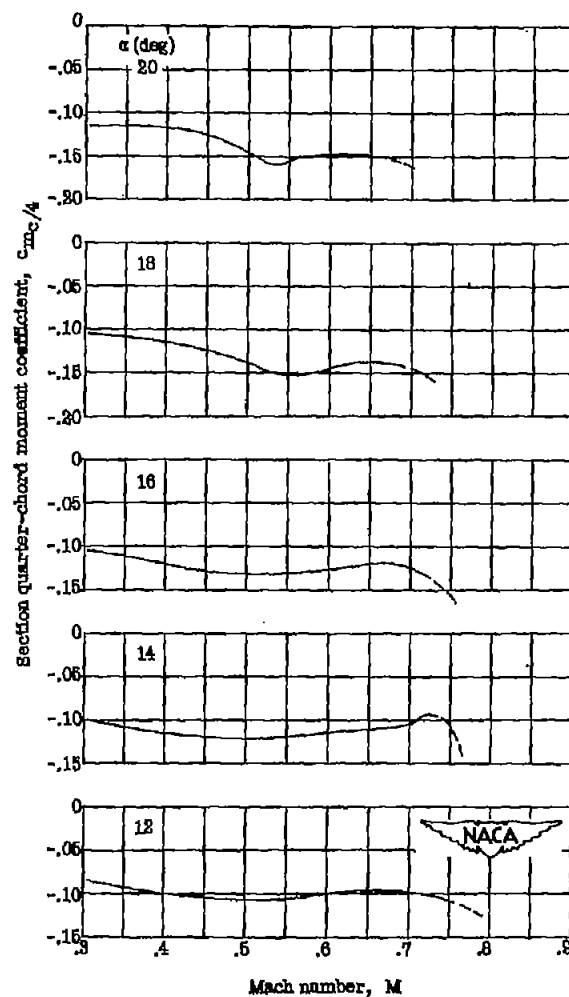
14
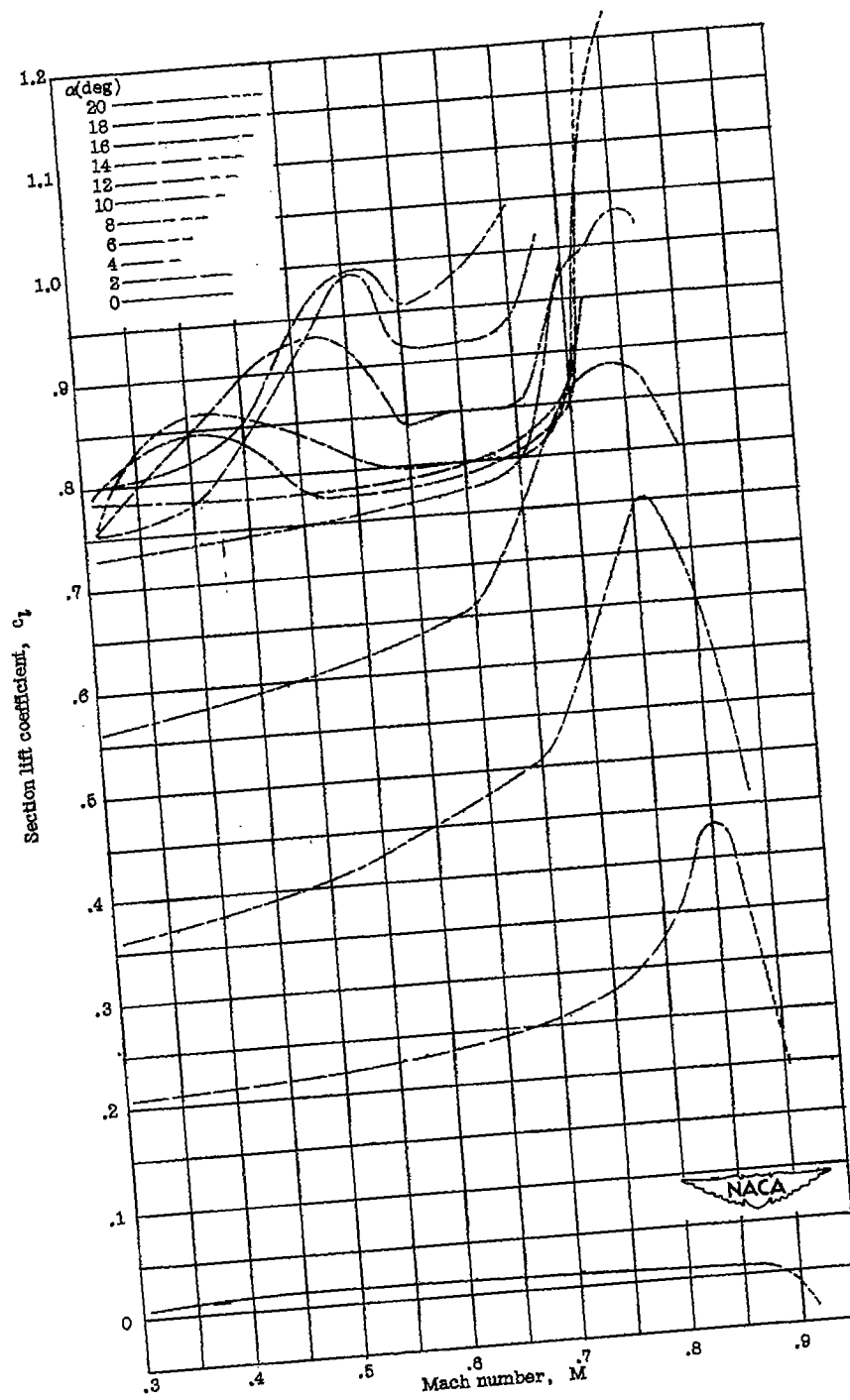
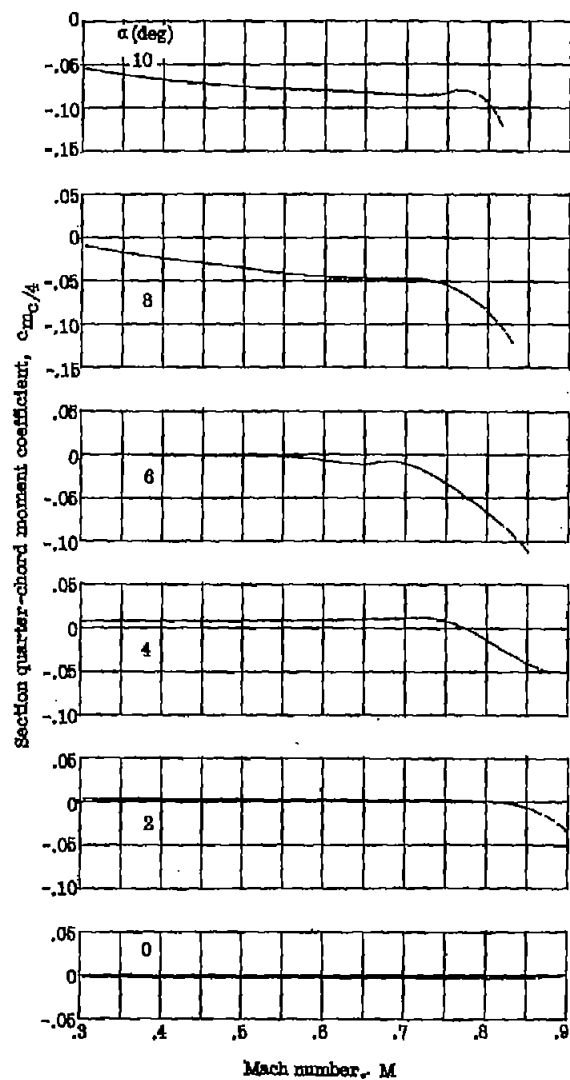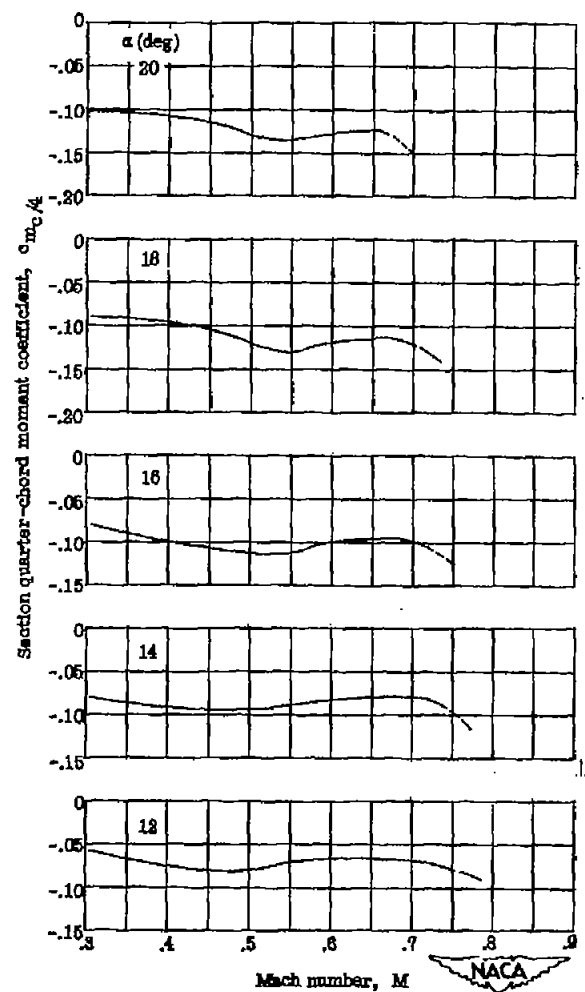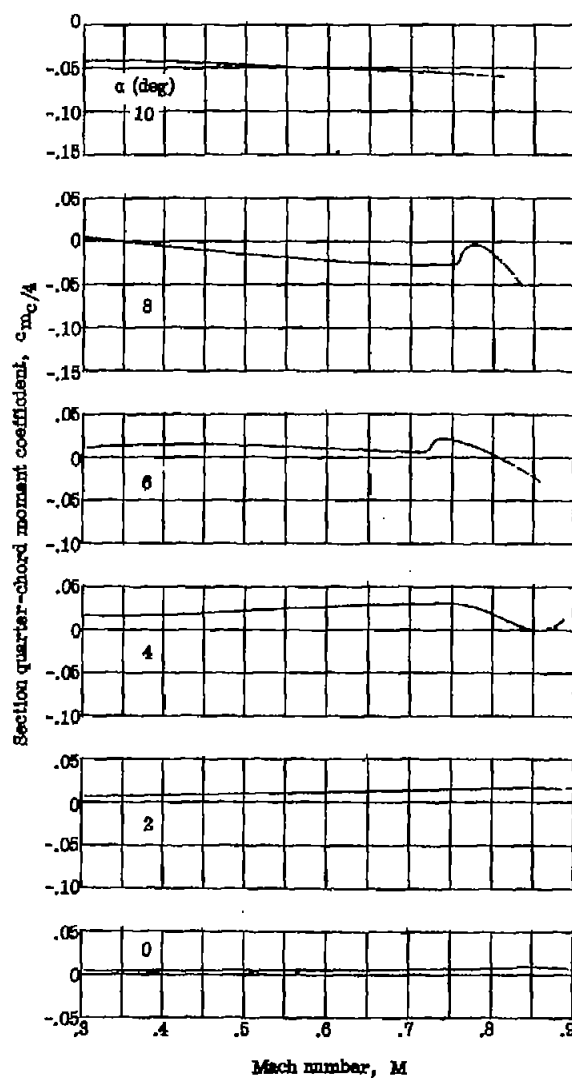
(b) NACA 66-006 airfoil.

Figure 3.— Continued.
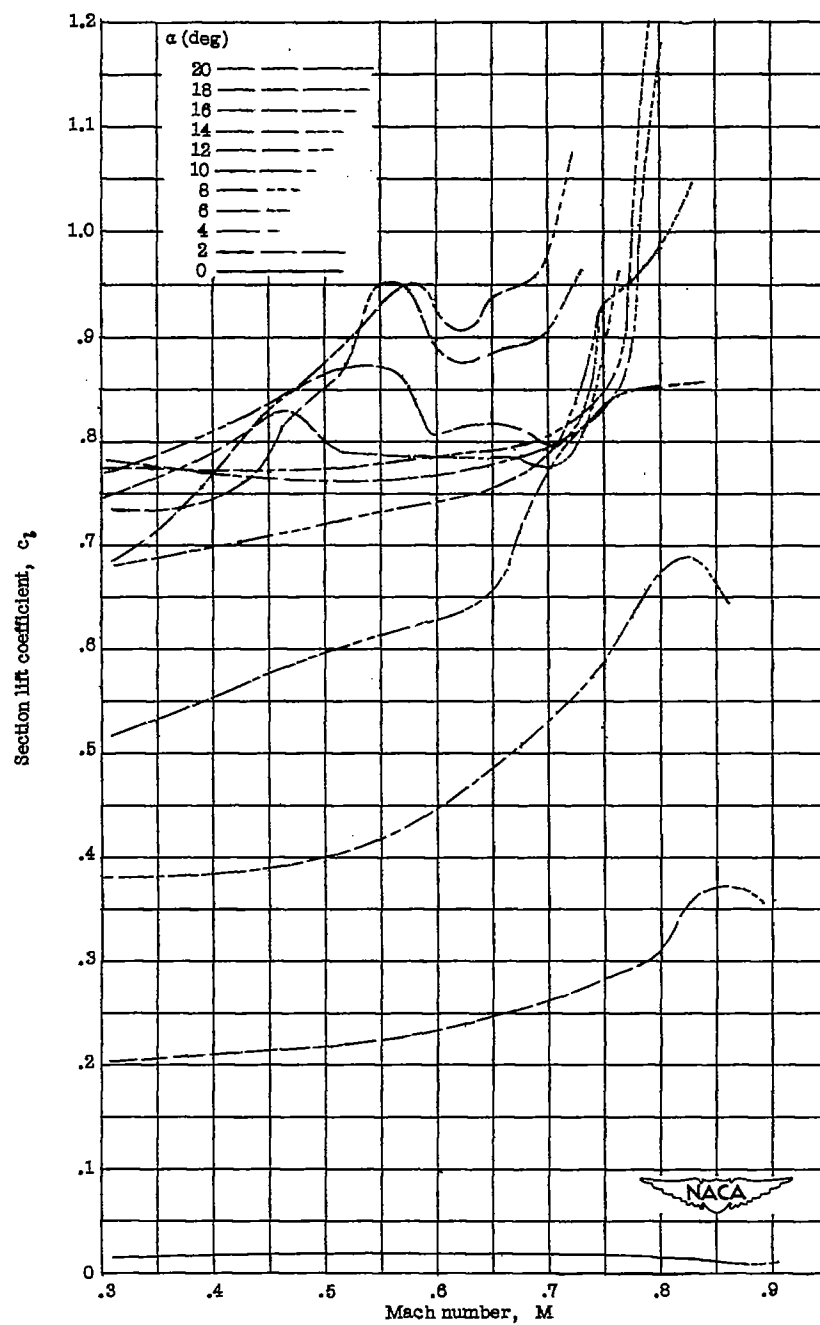
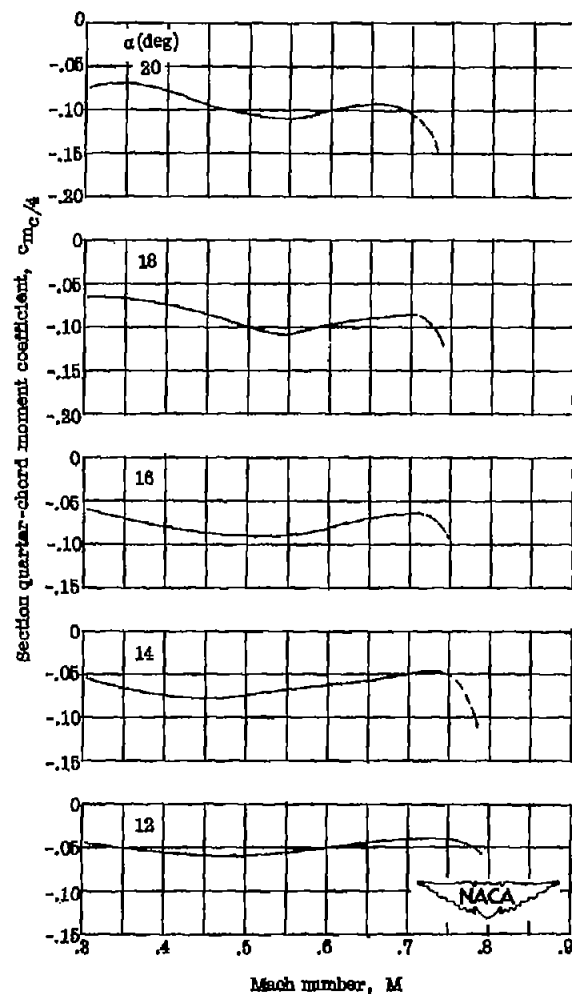(c) NACA 0006–63 airfoil.
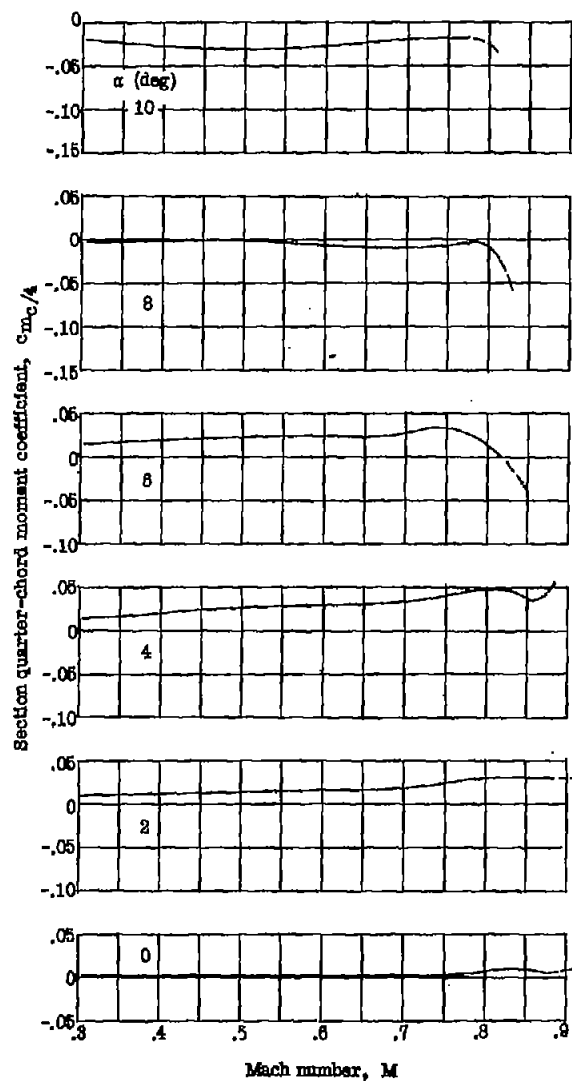
Figure 3.— Continued.
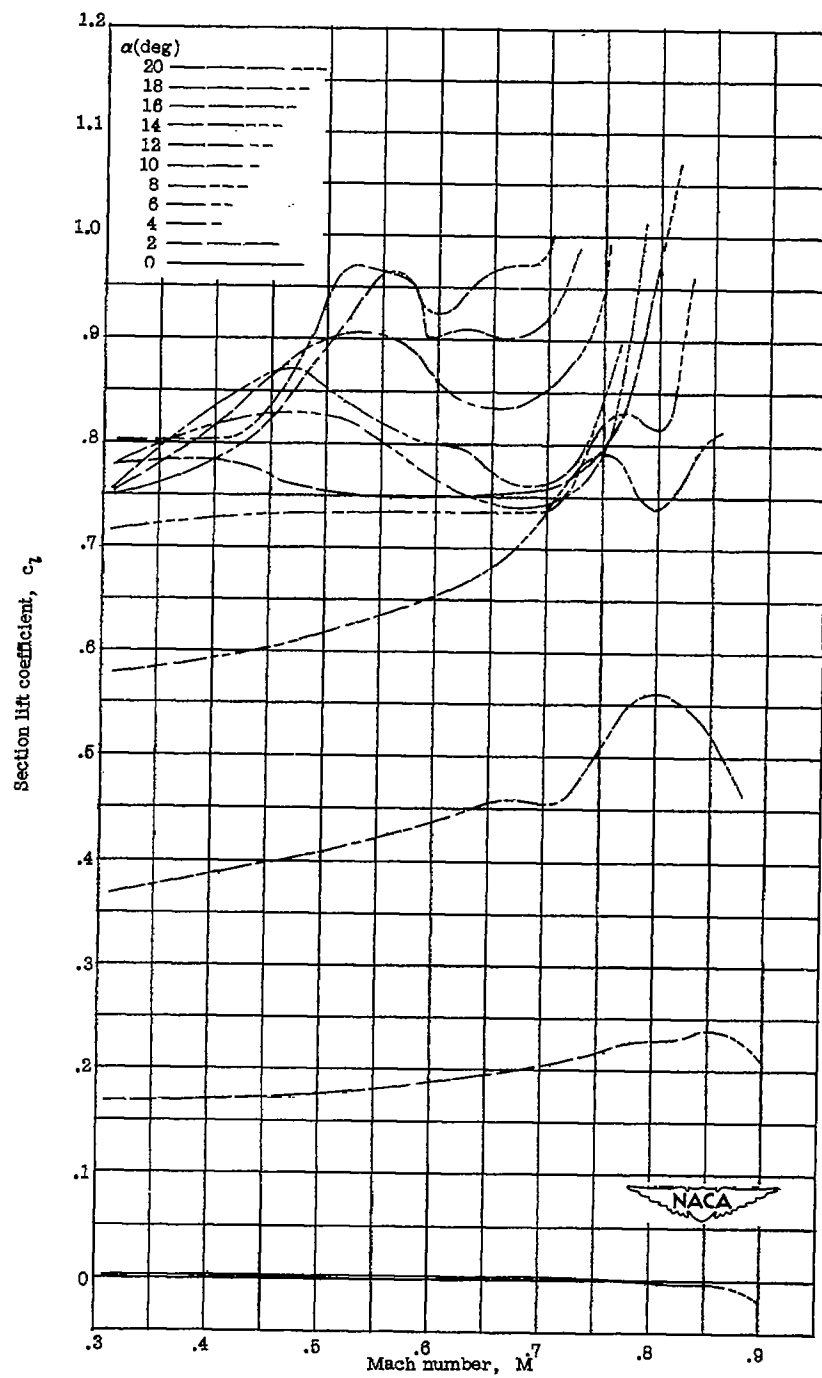
(d)   C–3 airfoil.
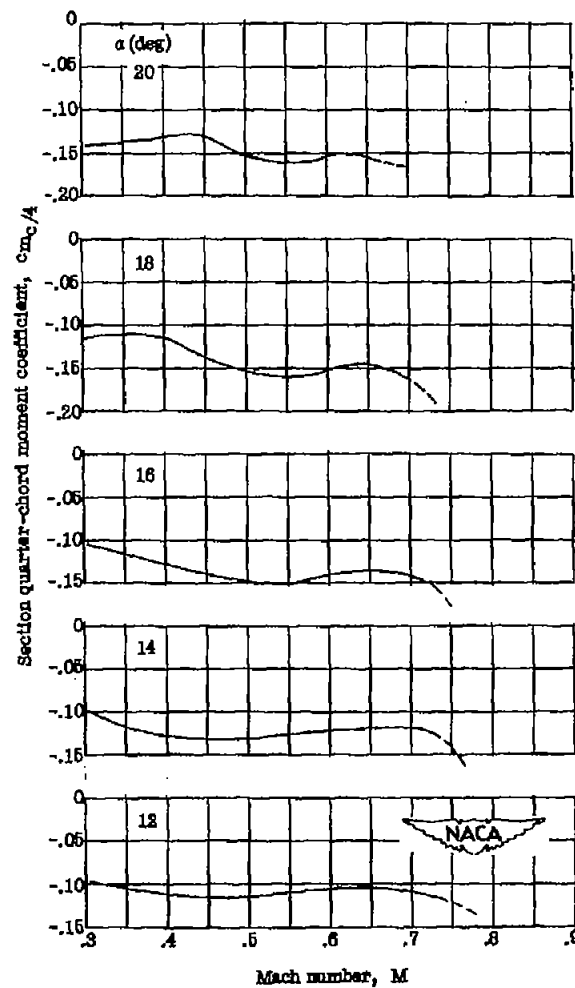
Figure 3.— Continued.
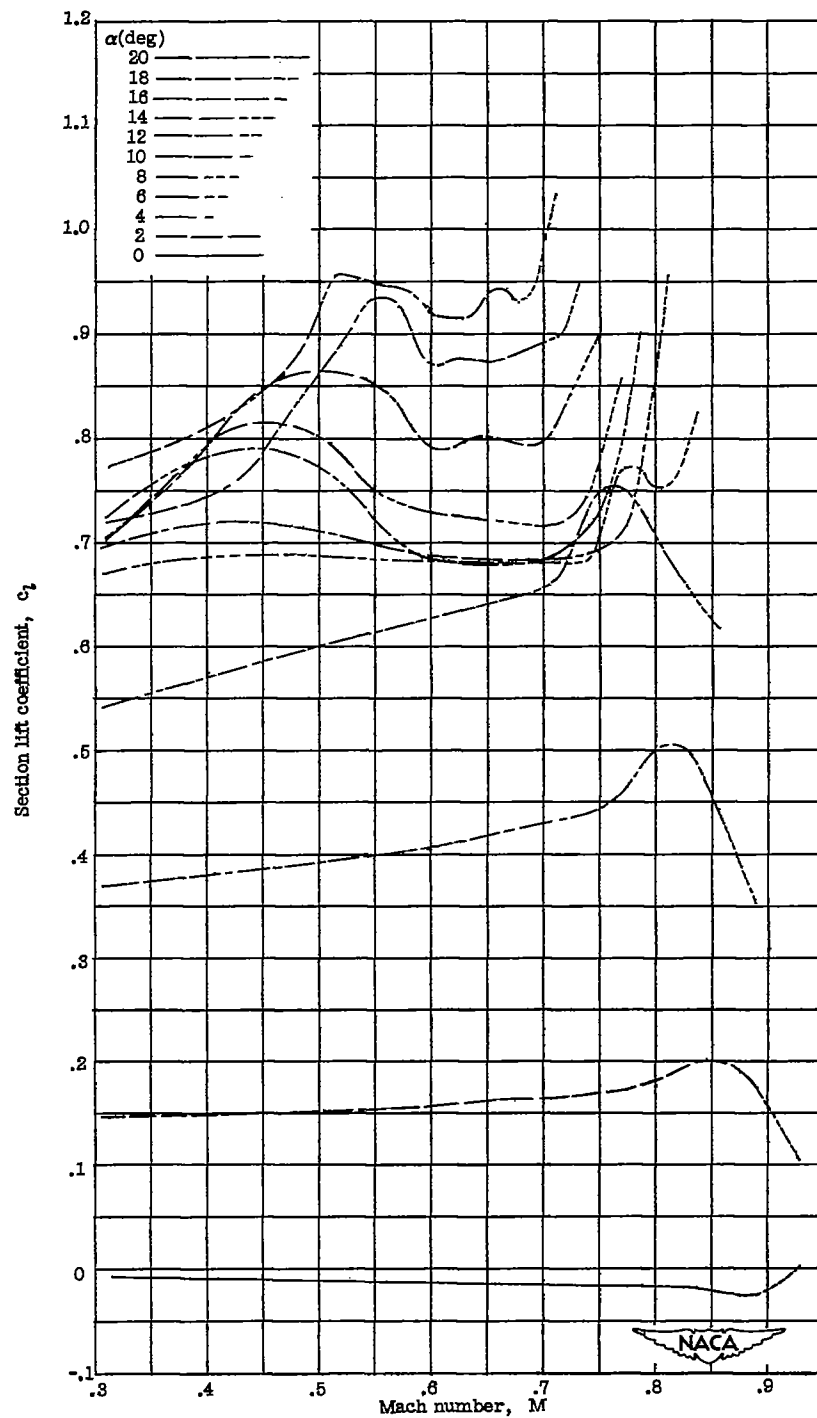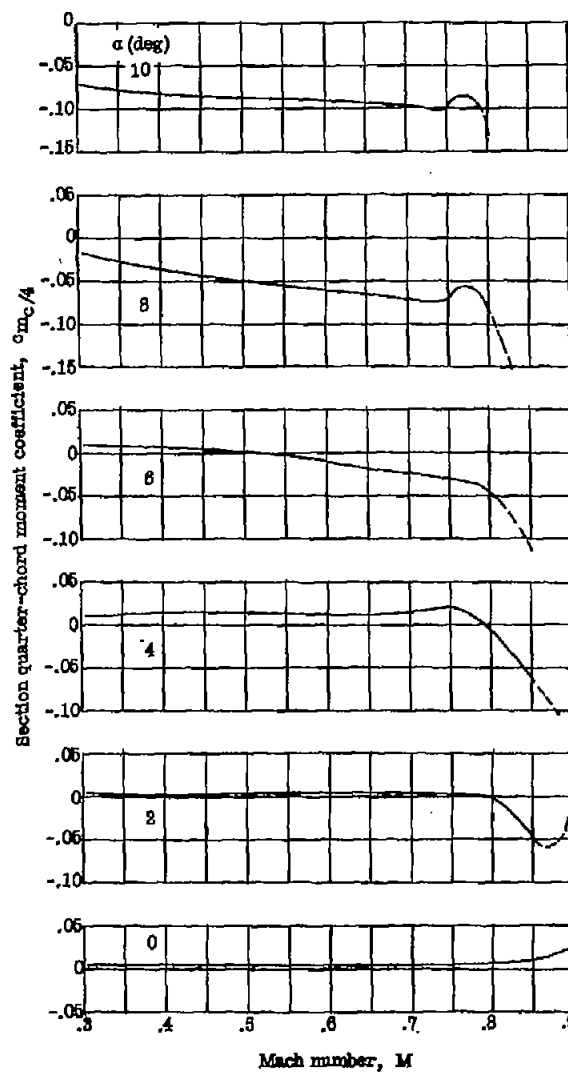
(e) C-5 airfoil.

Figure 3.— Continued.
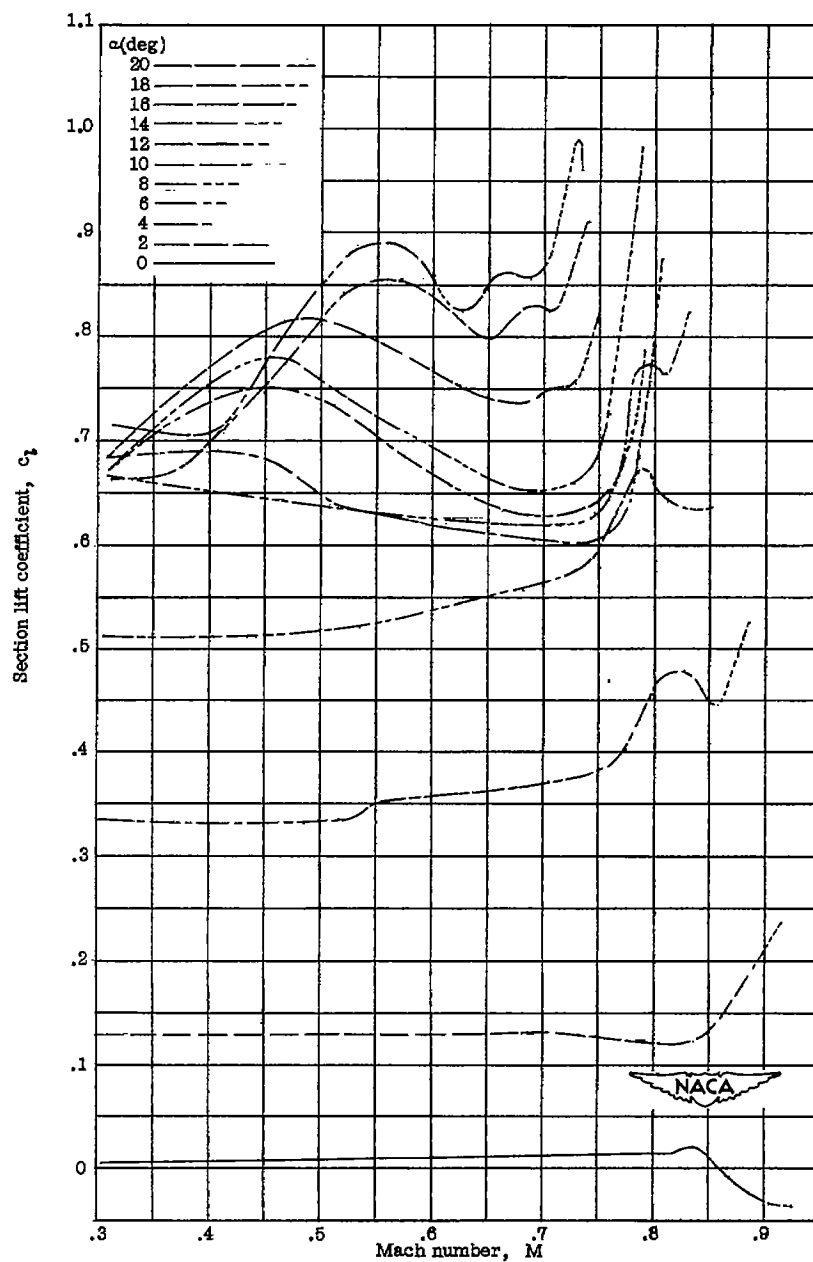
(f)   C-7 airfoil.

Figure 3.— Continued.
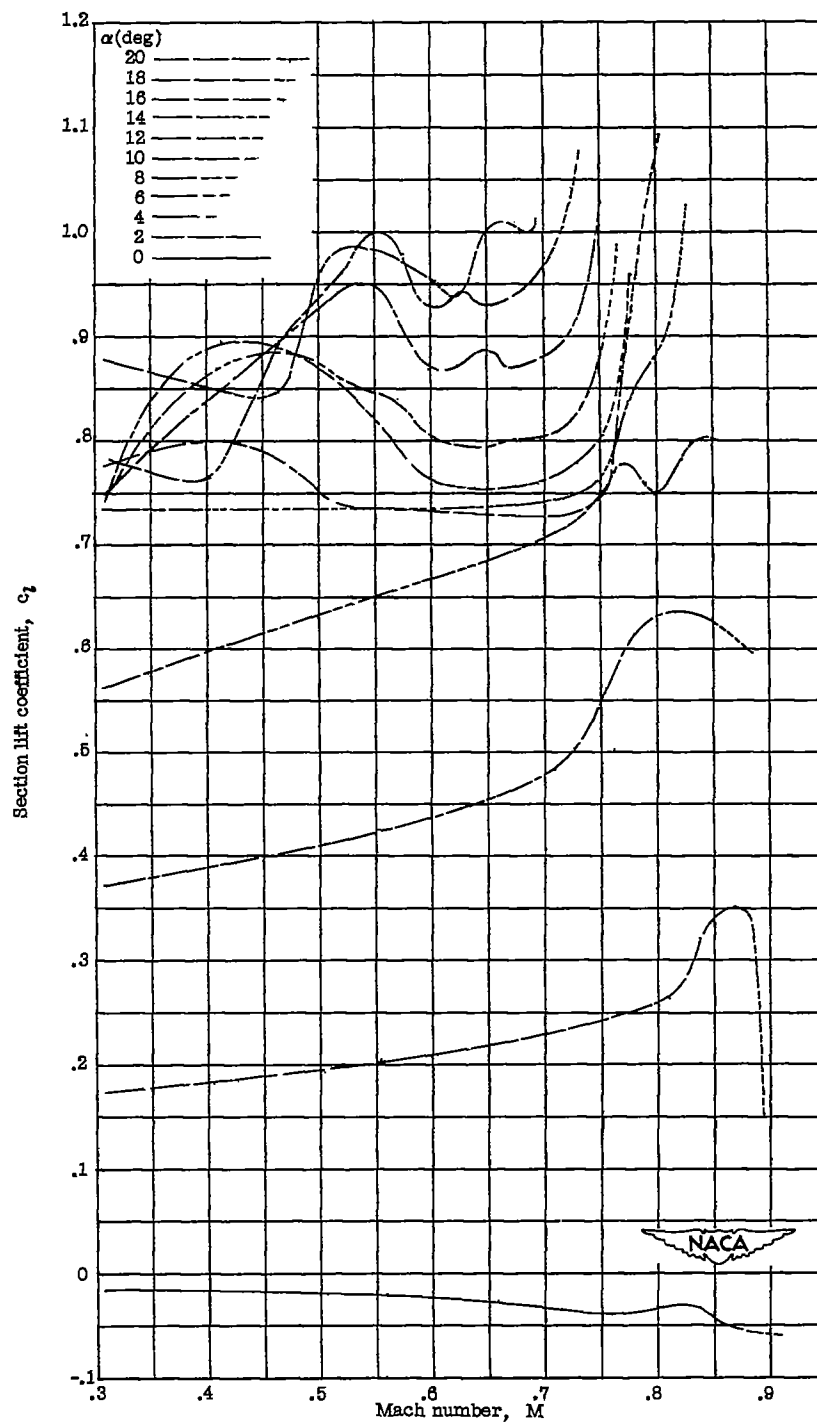
(g) W—3 airfoil.

Figure 3.— Continued.
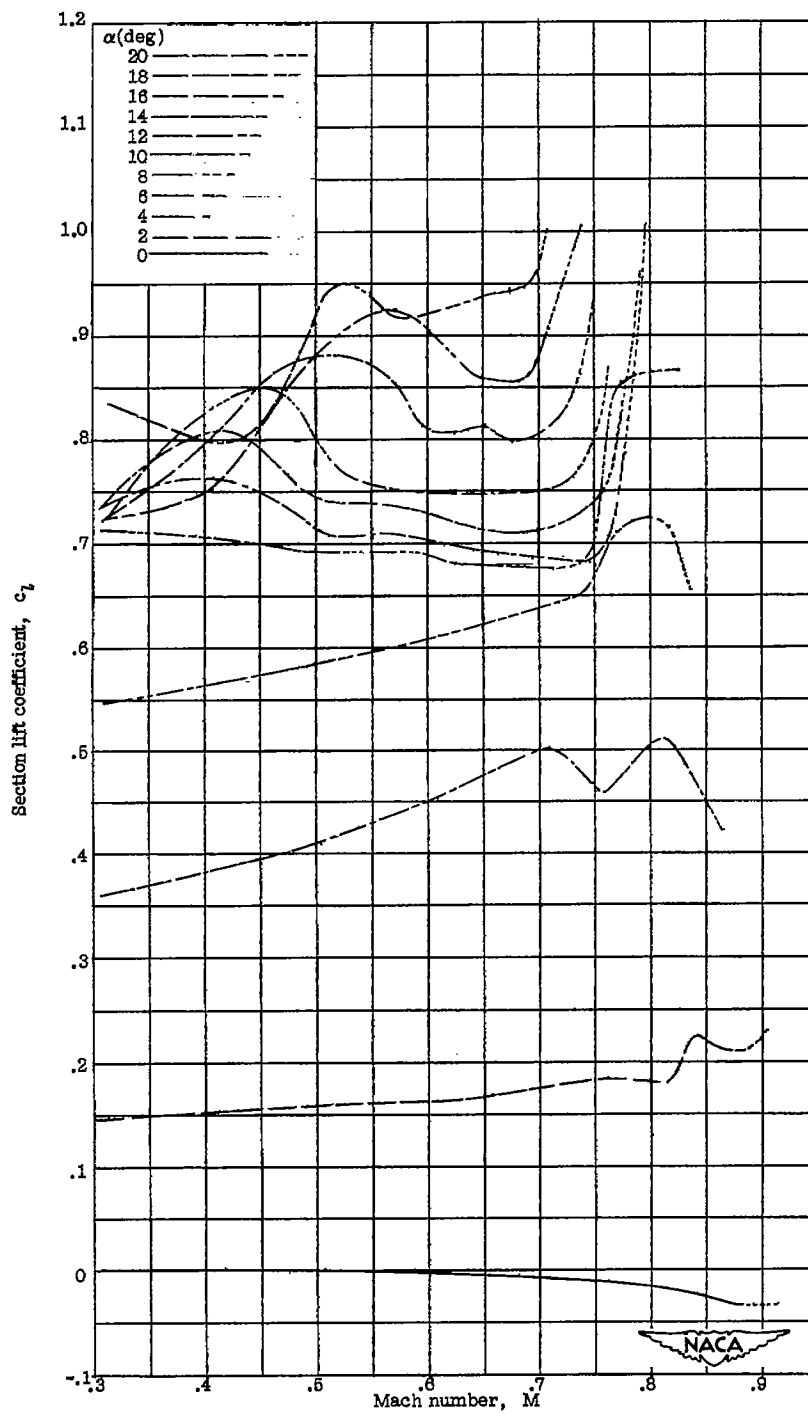
(h) W-7 airfoil.

Figure 3.— Concluded.

(a)   NACA 16-006 airfoil.

(b)   NACA 66-006 airfoil.
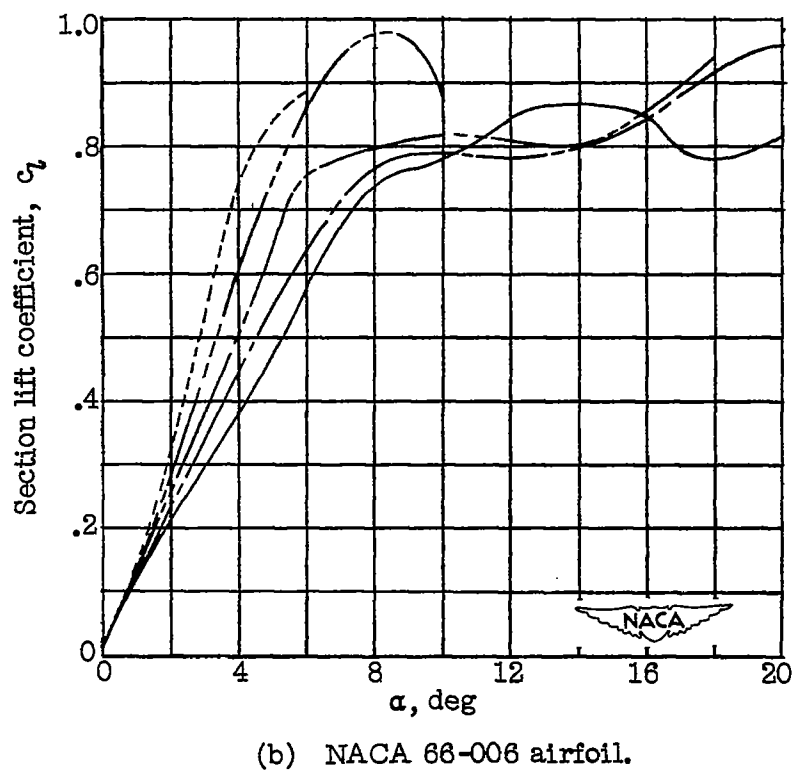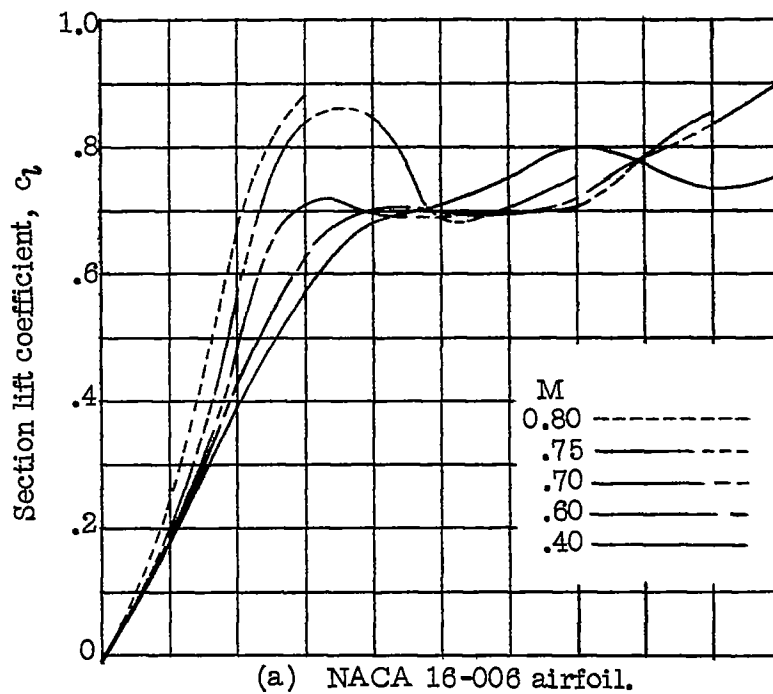
Figure 4.— Variation of section lift coefficient c_l with angle of
attack α.

(c)   NACA 0006-63 airfoil.

(d)   C-3 airfoil.

Figure 4.— Continued.

(e) C-5 airfoil.
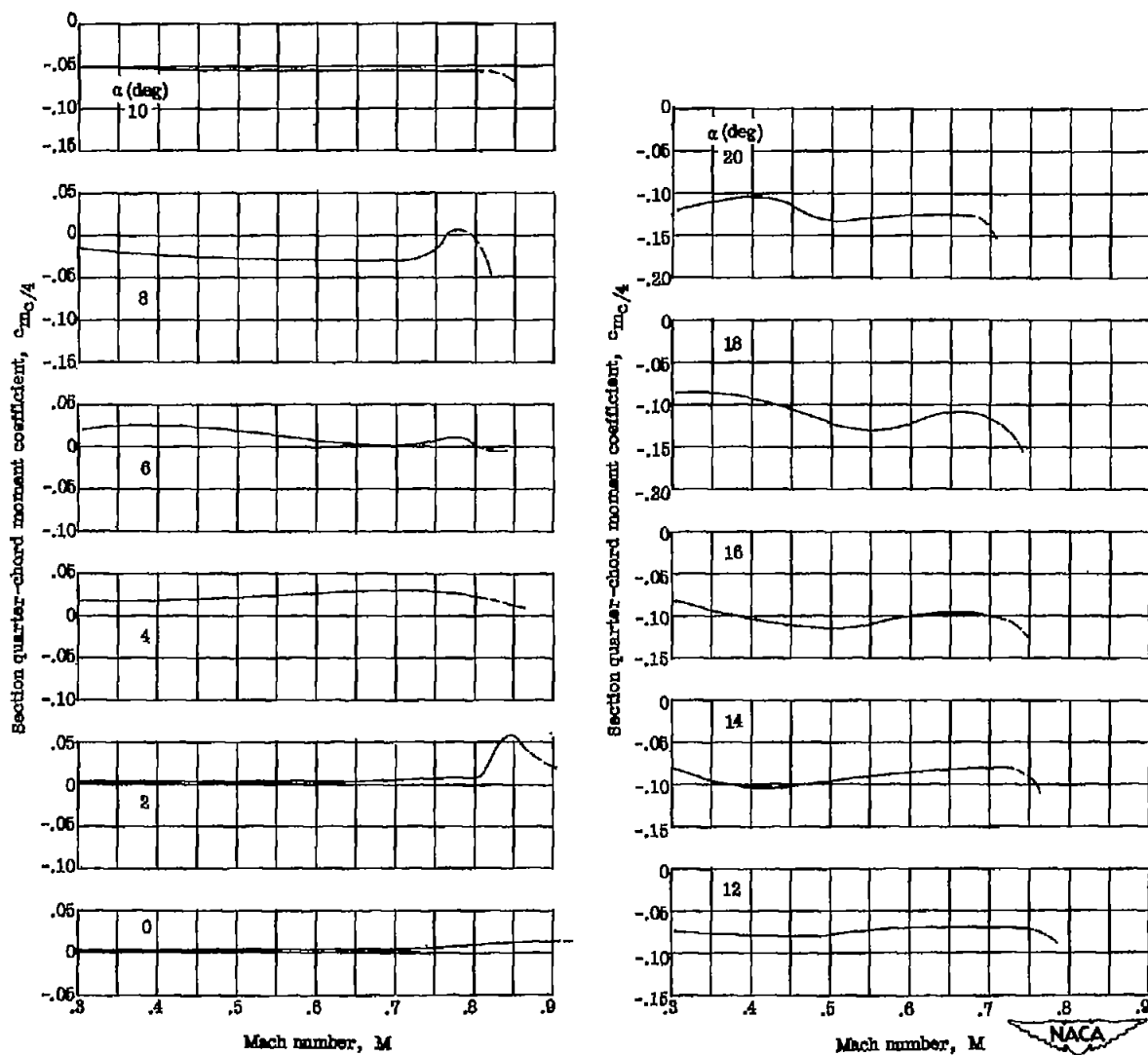
(f) C-7 airfoil.

Figure 4.— Continued.

(g) W-3 airfoil.

(h) W-7 airfoil.
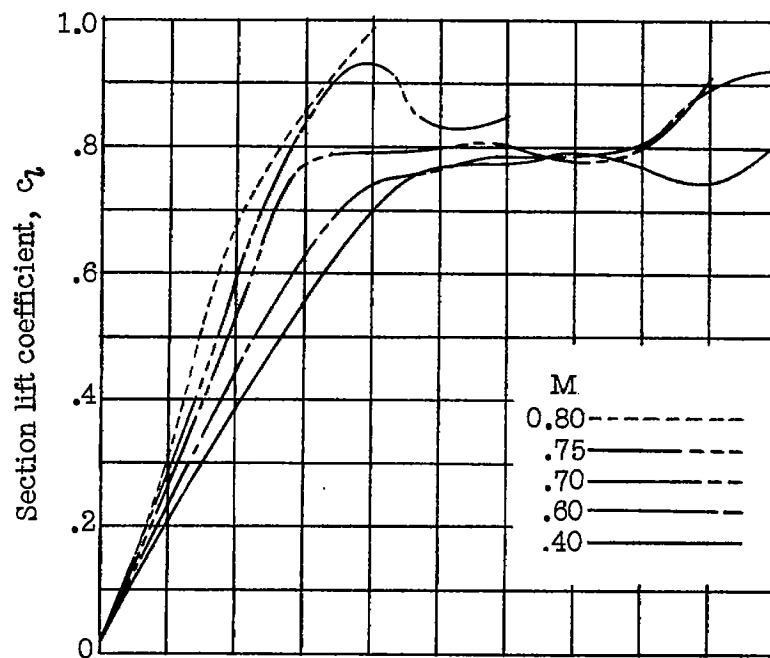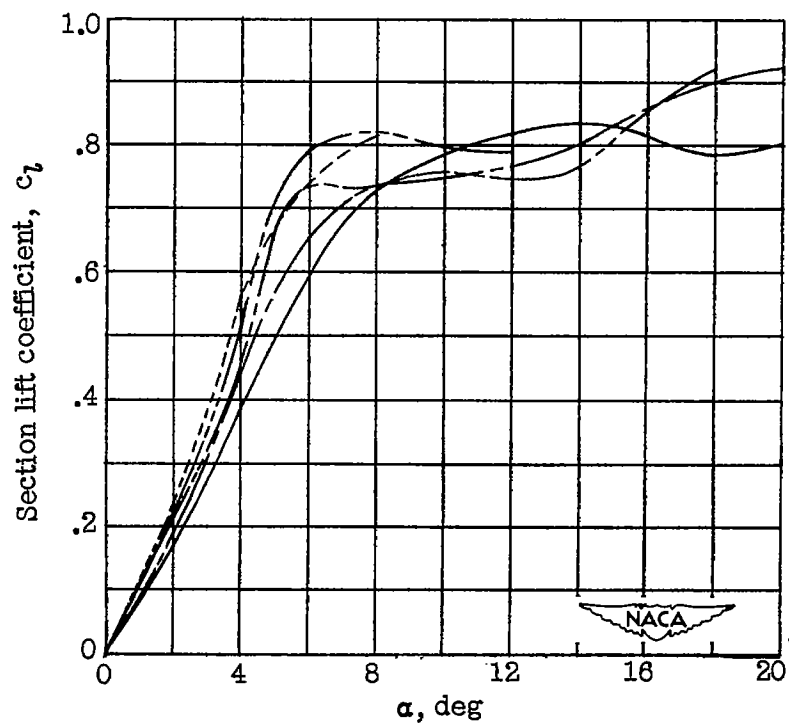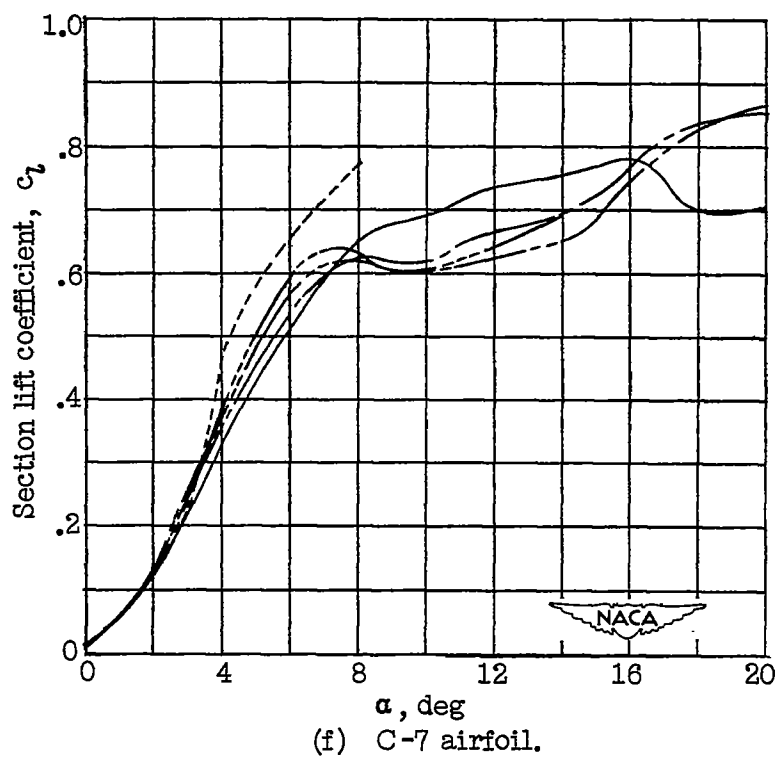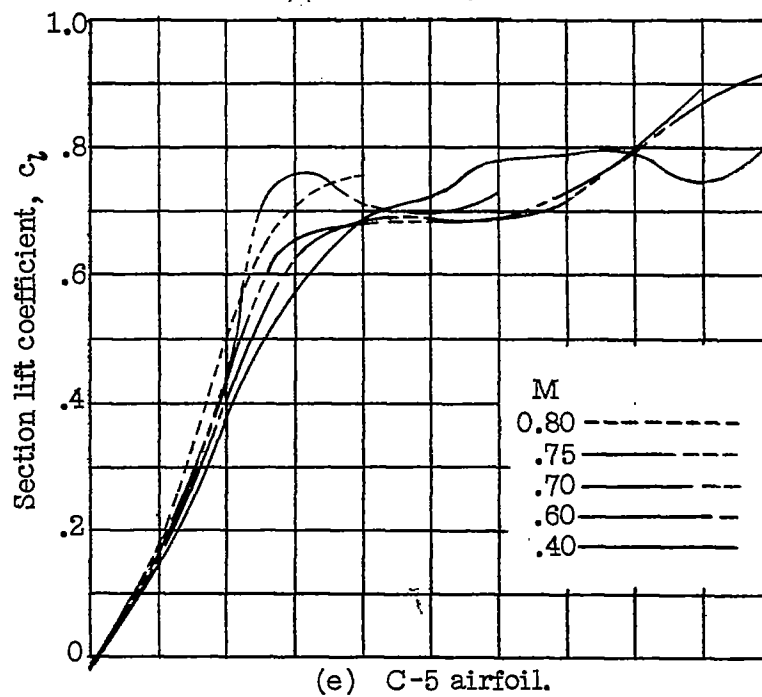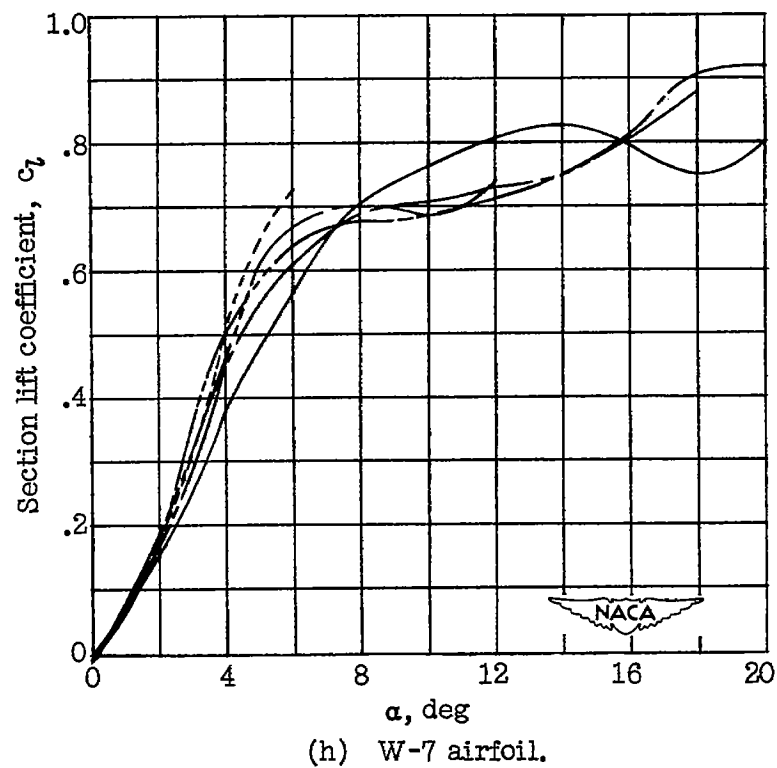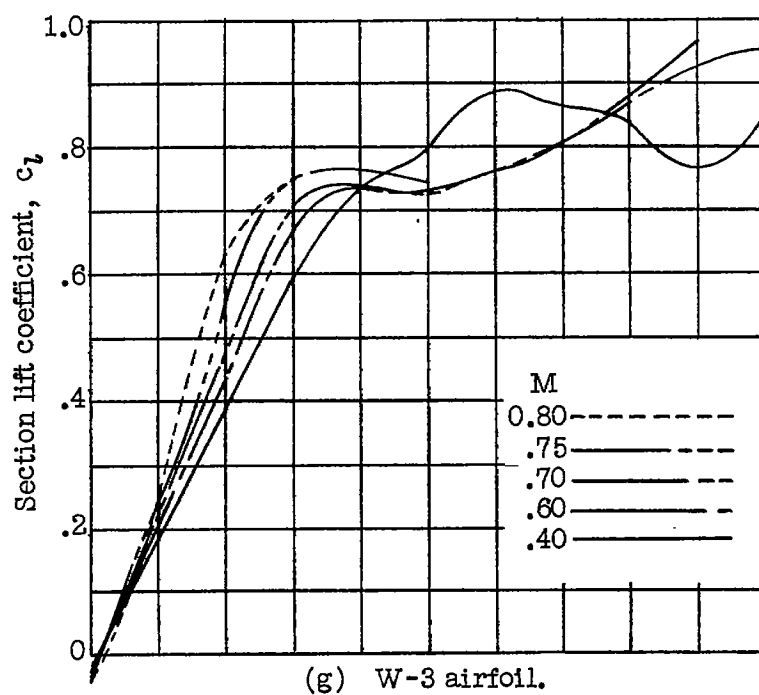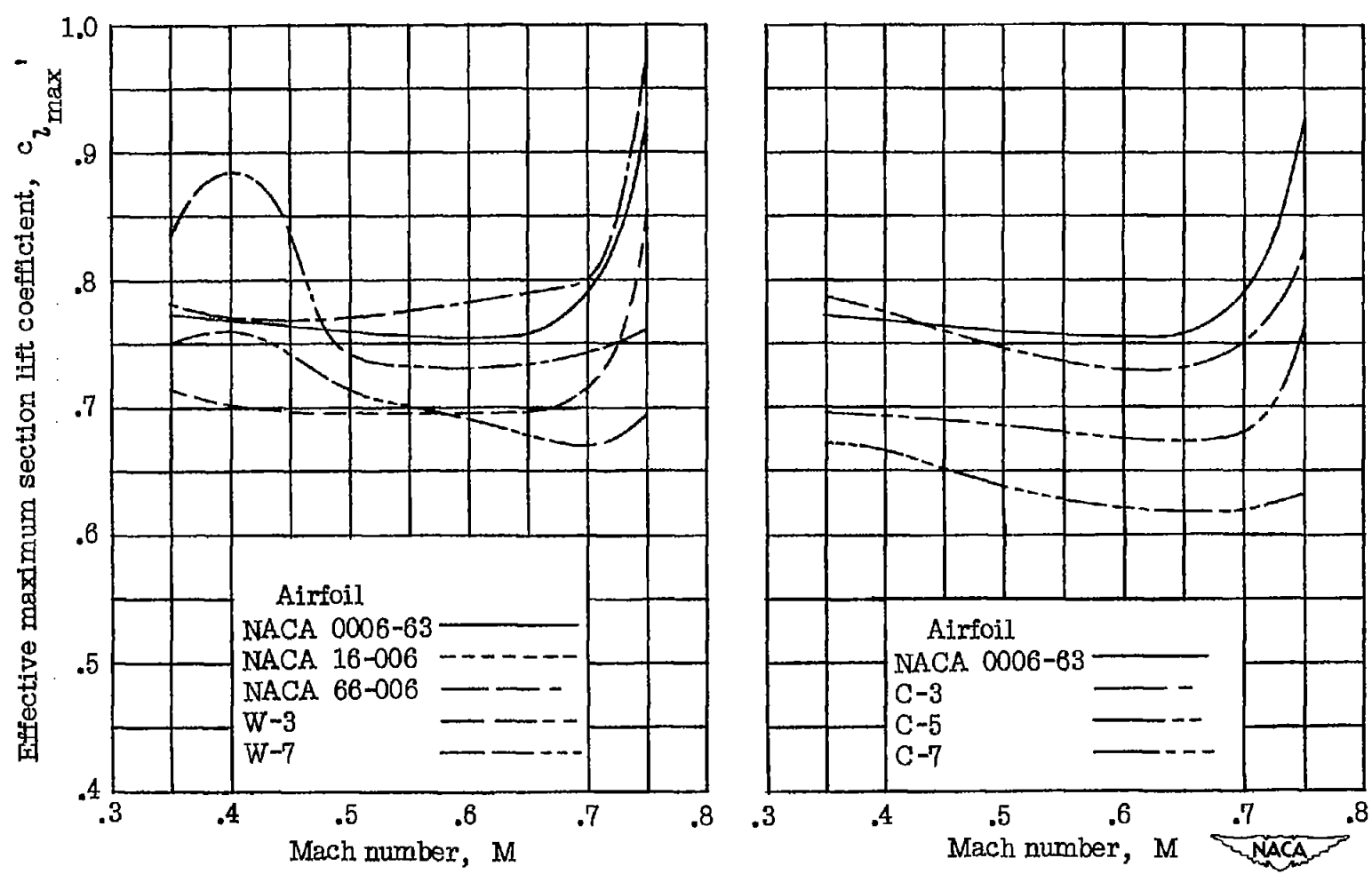
Figure 4.— Concluded.

(a) Effect of Mach number.

Figure 5.— Effective-maximum-section-lift-coefficient characteristics.
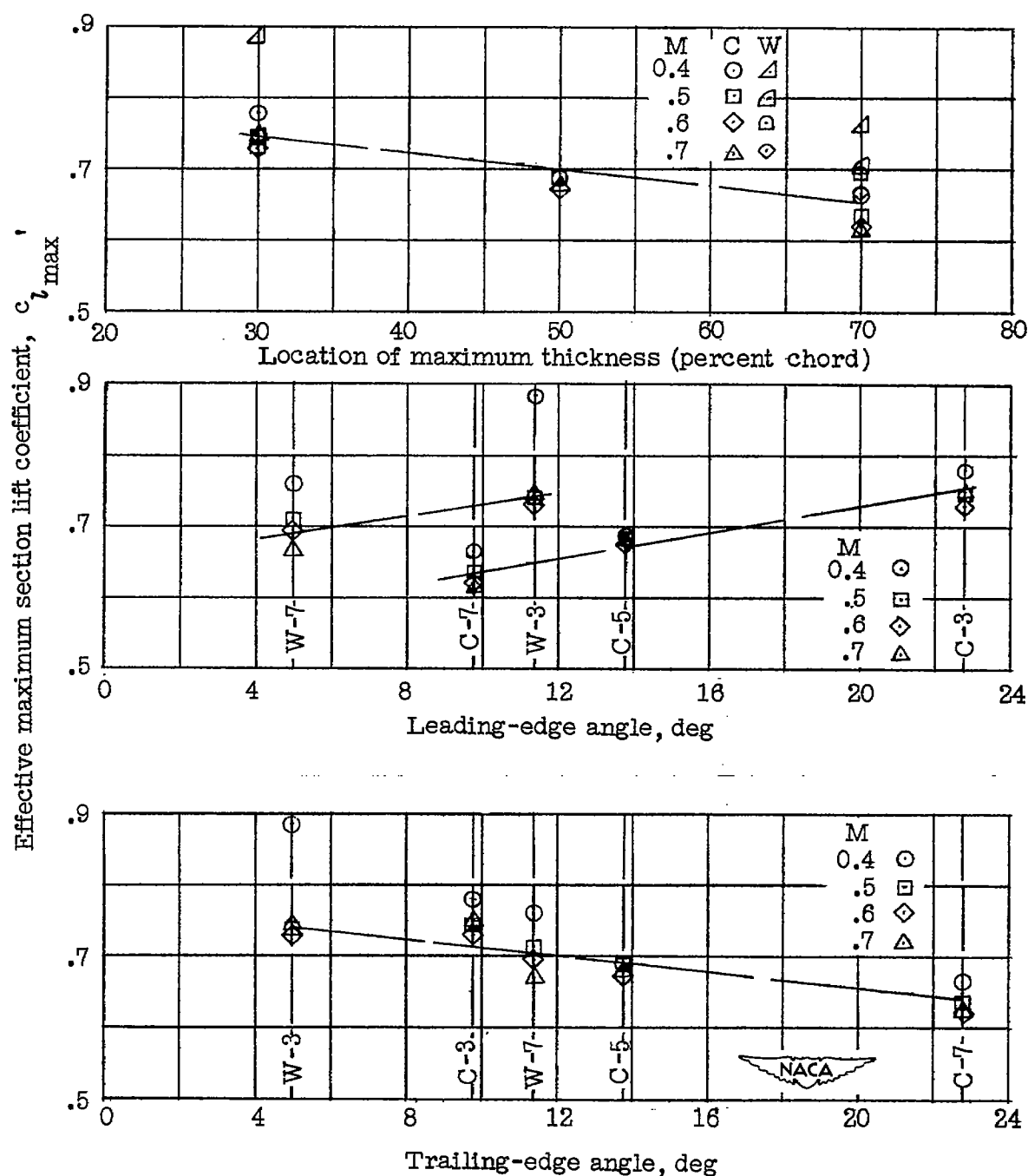
(b) Effect of maximum-thickness location, leading-edge angle, and trailing-edge angle.

Figure 5.— Concluded.
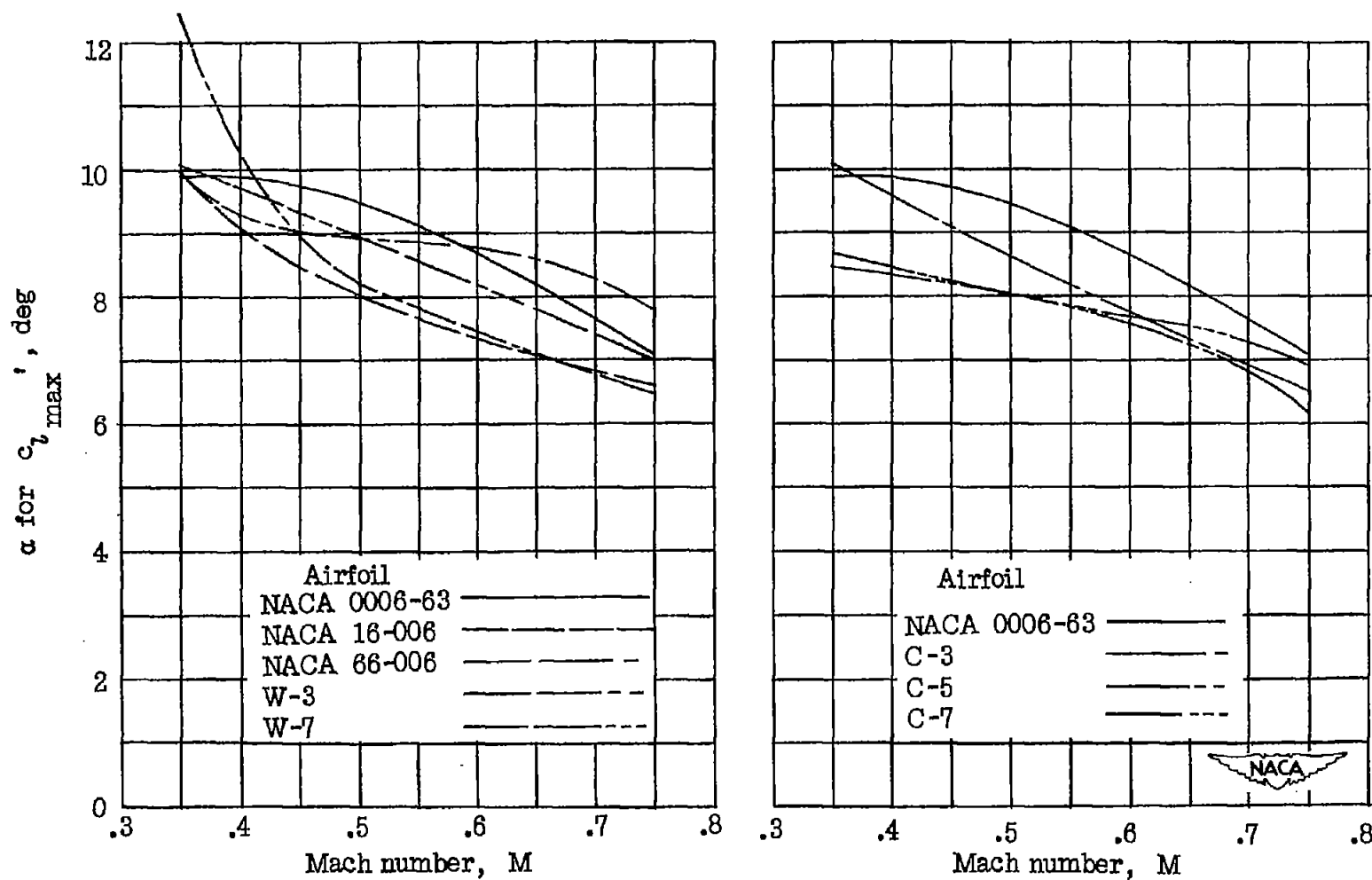
Figure 6.— Variation of angle of attack for effective maximum section lift coefficient with Mach number.
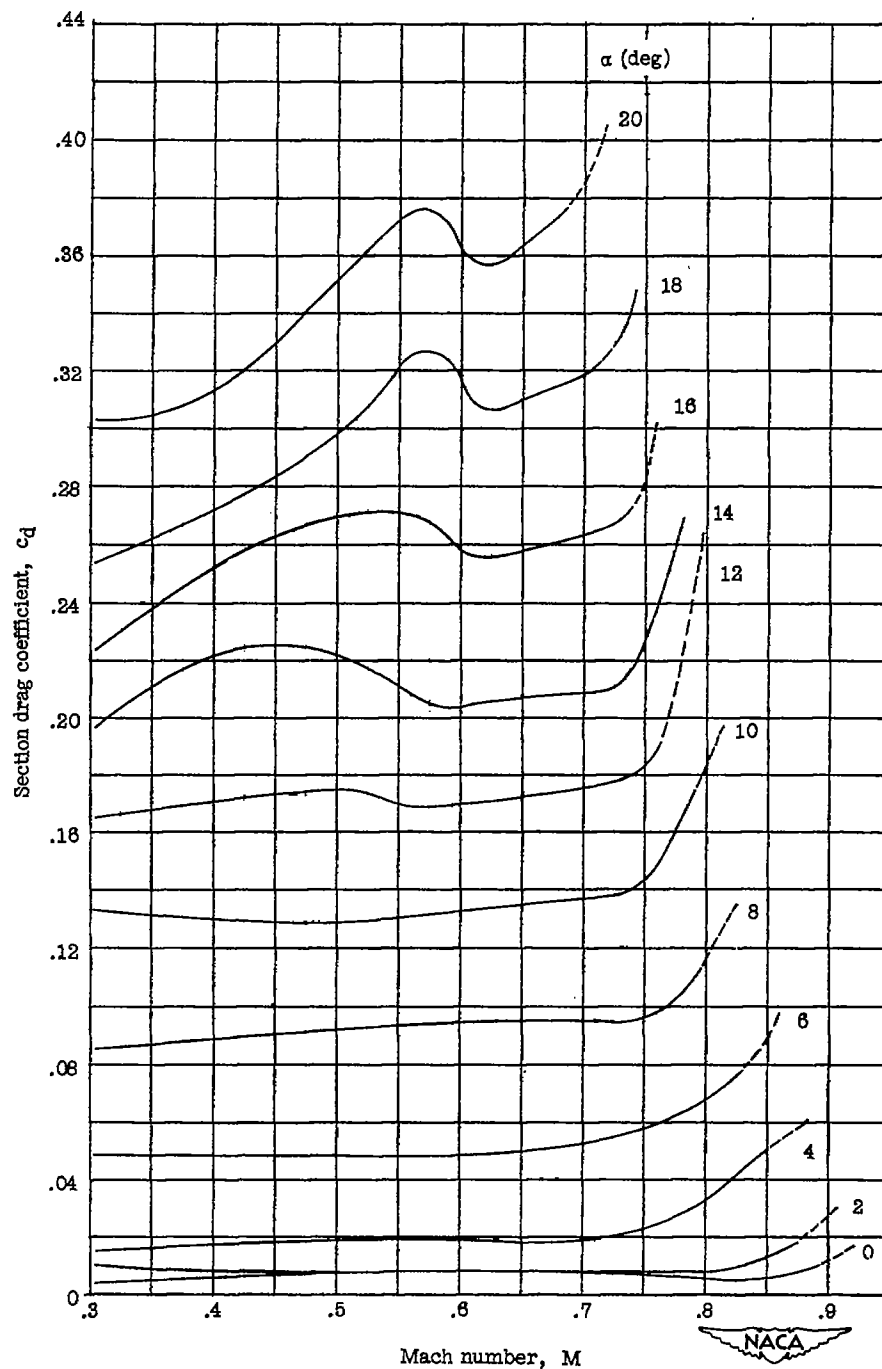
(a) NACA 16-006 airfoil.

Figure 7.- Variation of section drag coefficient c_d with Mach number M.
(Curves are dashed for data from $\left(M_{ch} - 0.030\right)$ to M_{ch}.)
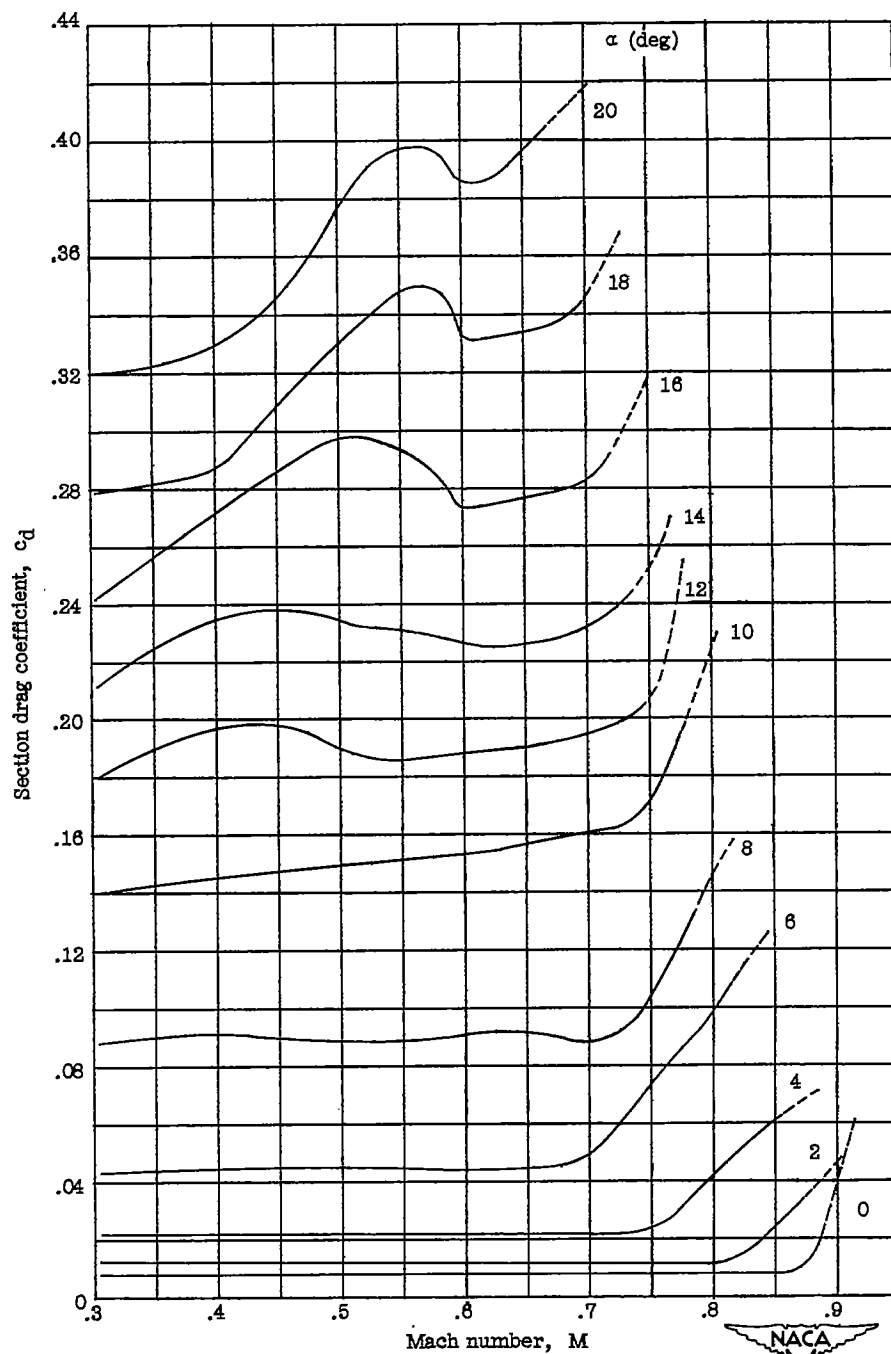
(b) NACA 66-006 airfoil.

Figure 7.— Continued.
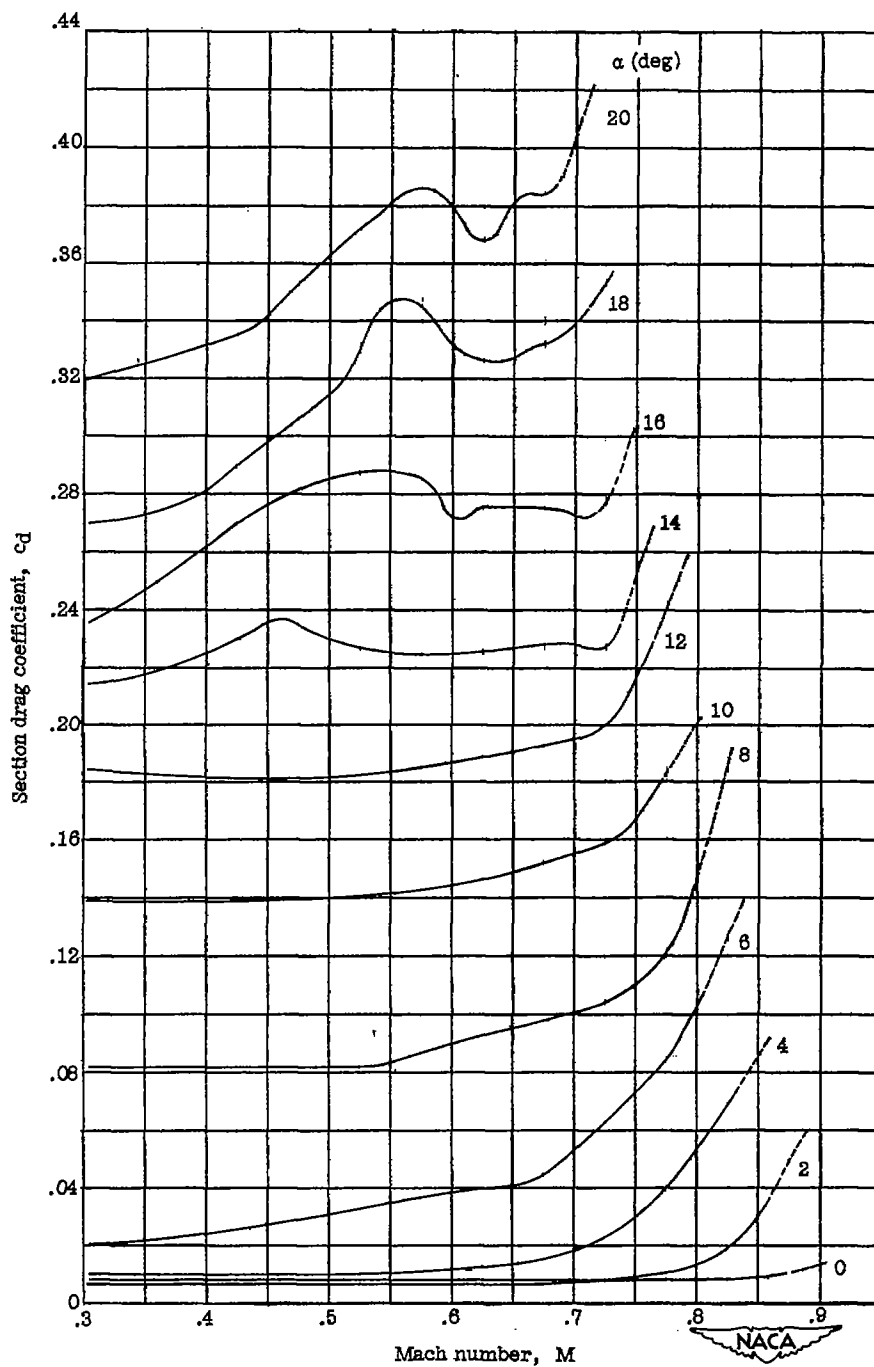
(c) NACA 0006-63 airfoil.

Figure 7.- Continued.
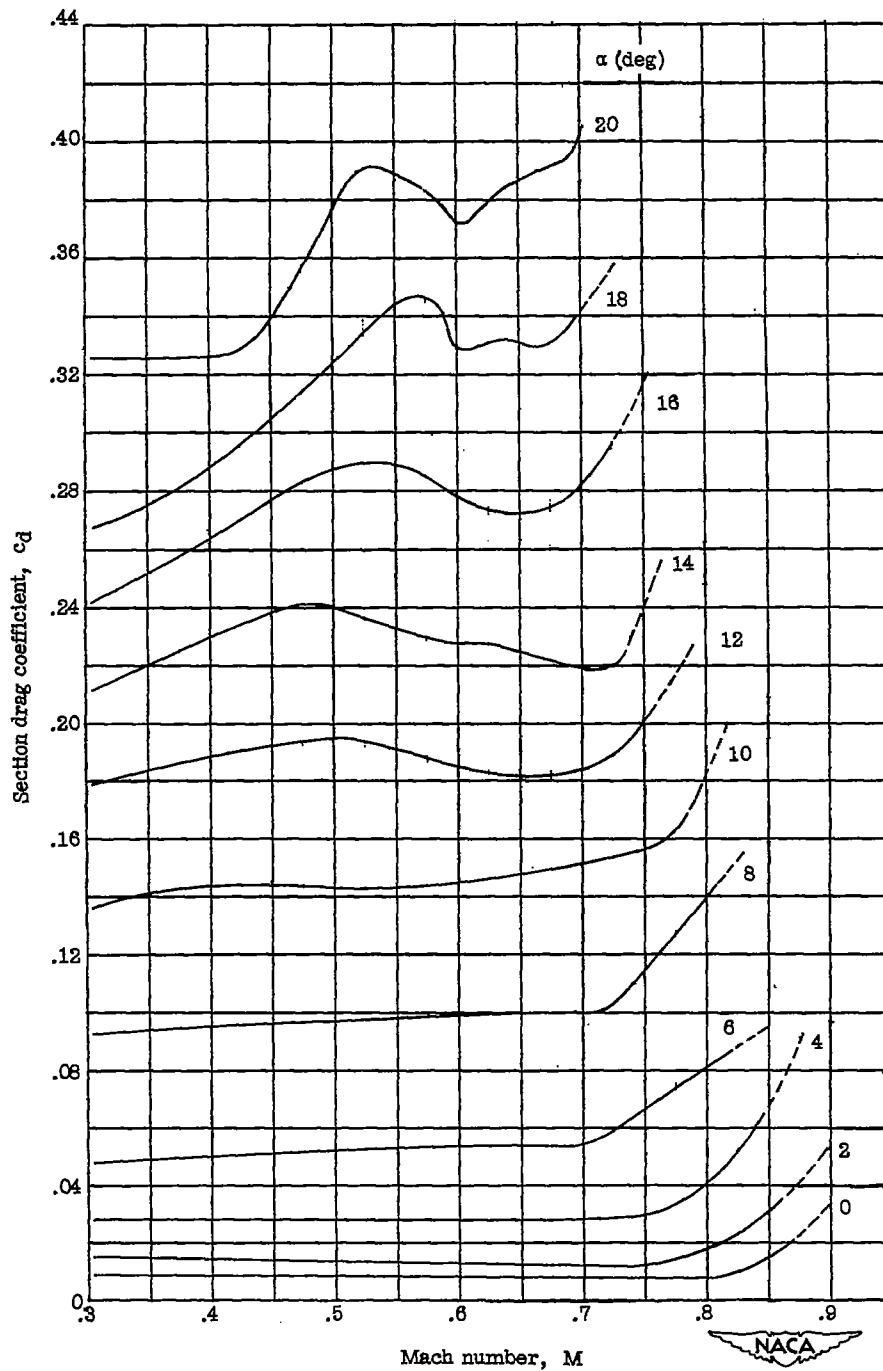
(d)   C—3 airfoil.

Figure 7.— Continued.
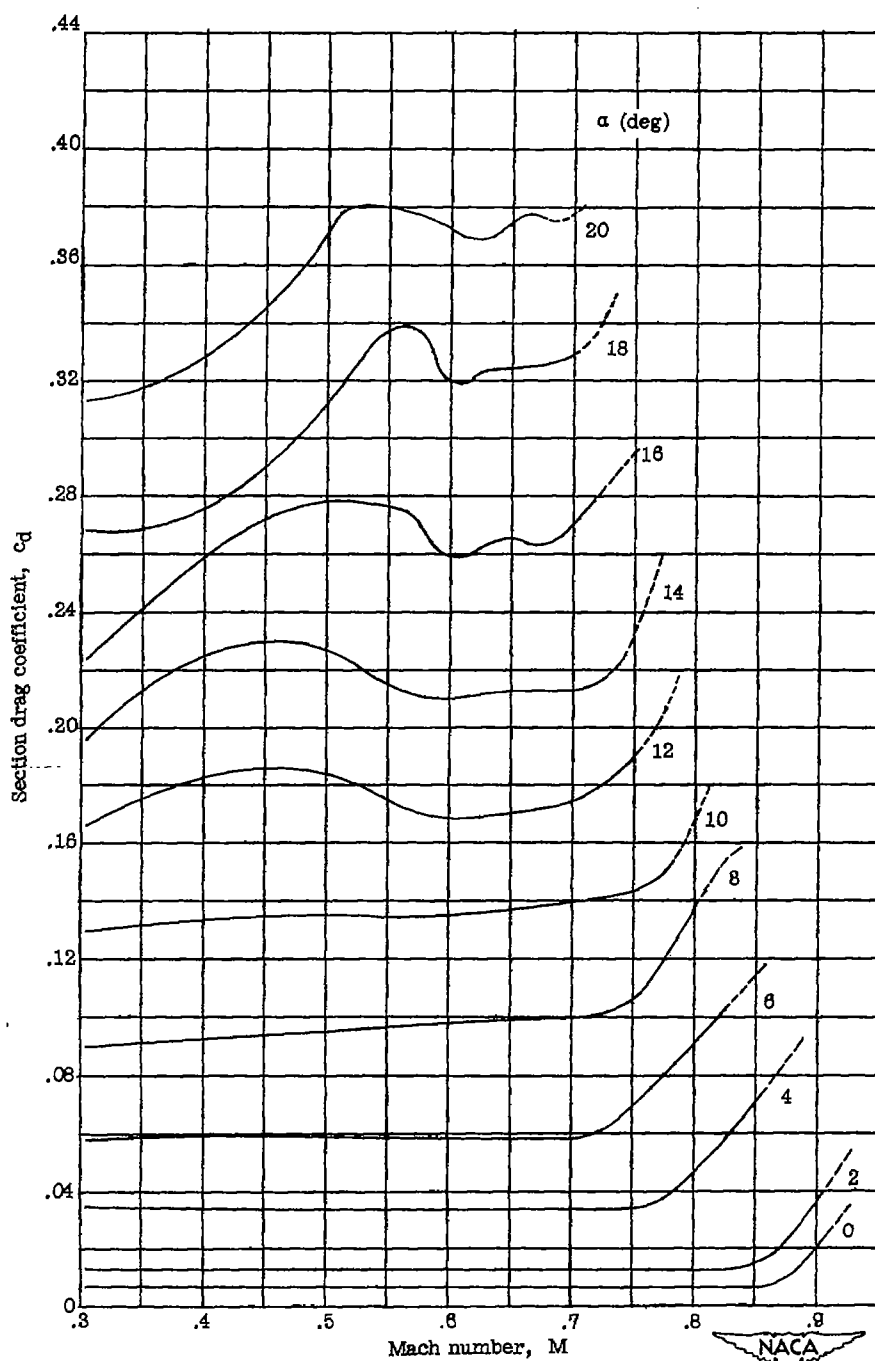
(e)   C-5 airfoil.

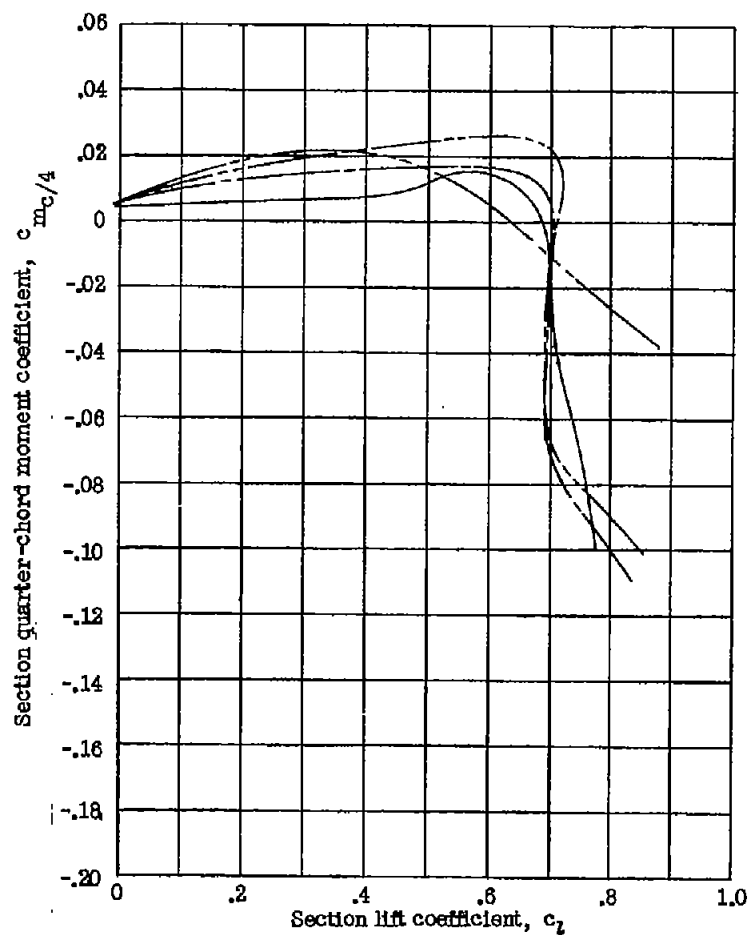Figure 7.— Continued.
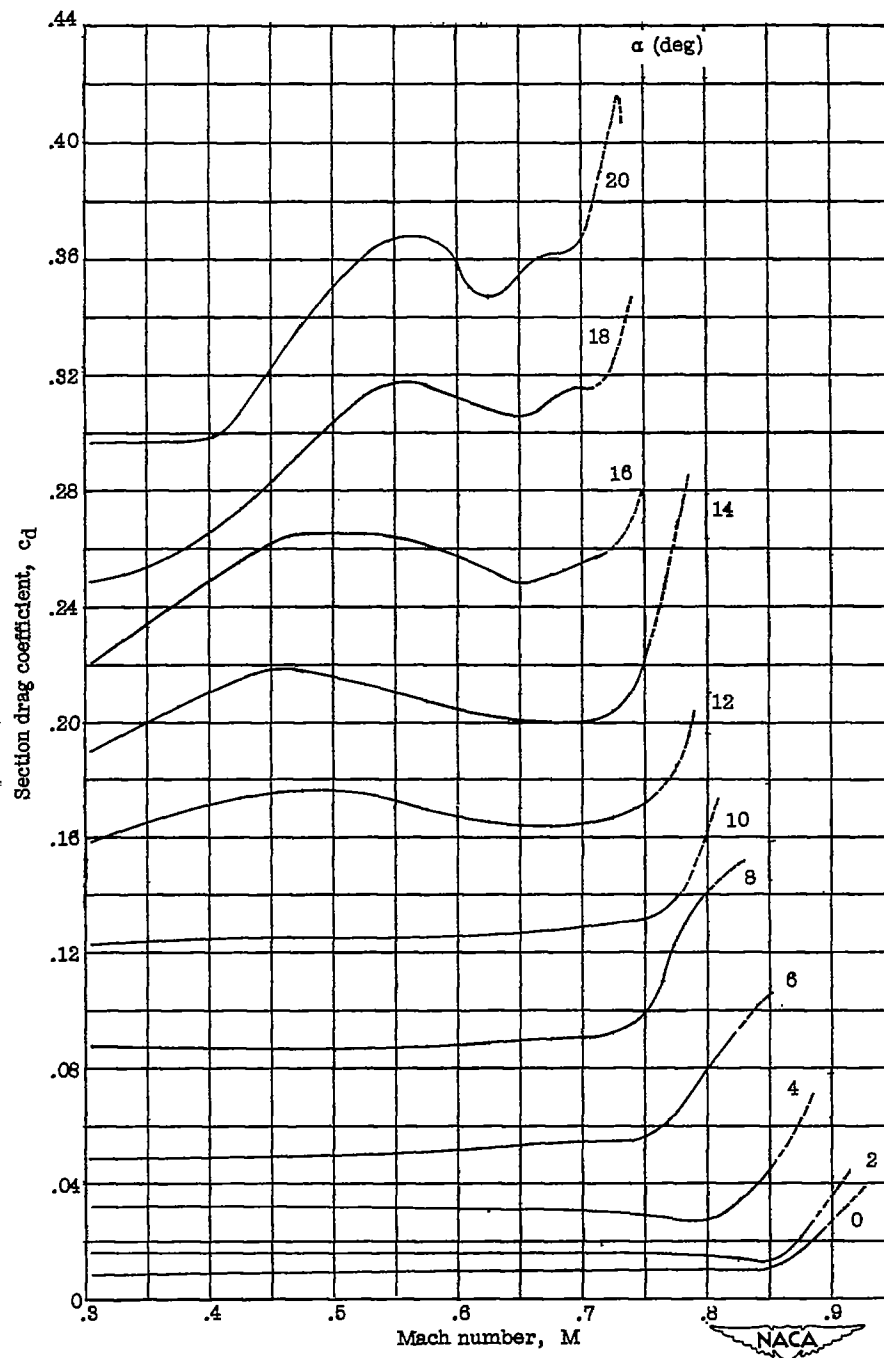
(f)   C-7 airfoil.

Figure 7.— Continued.
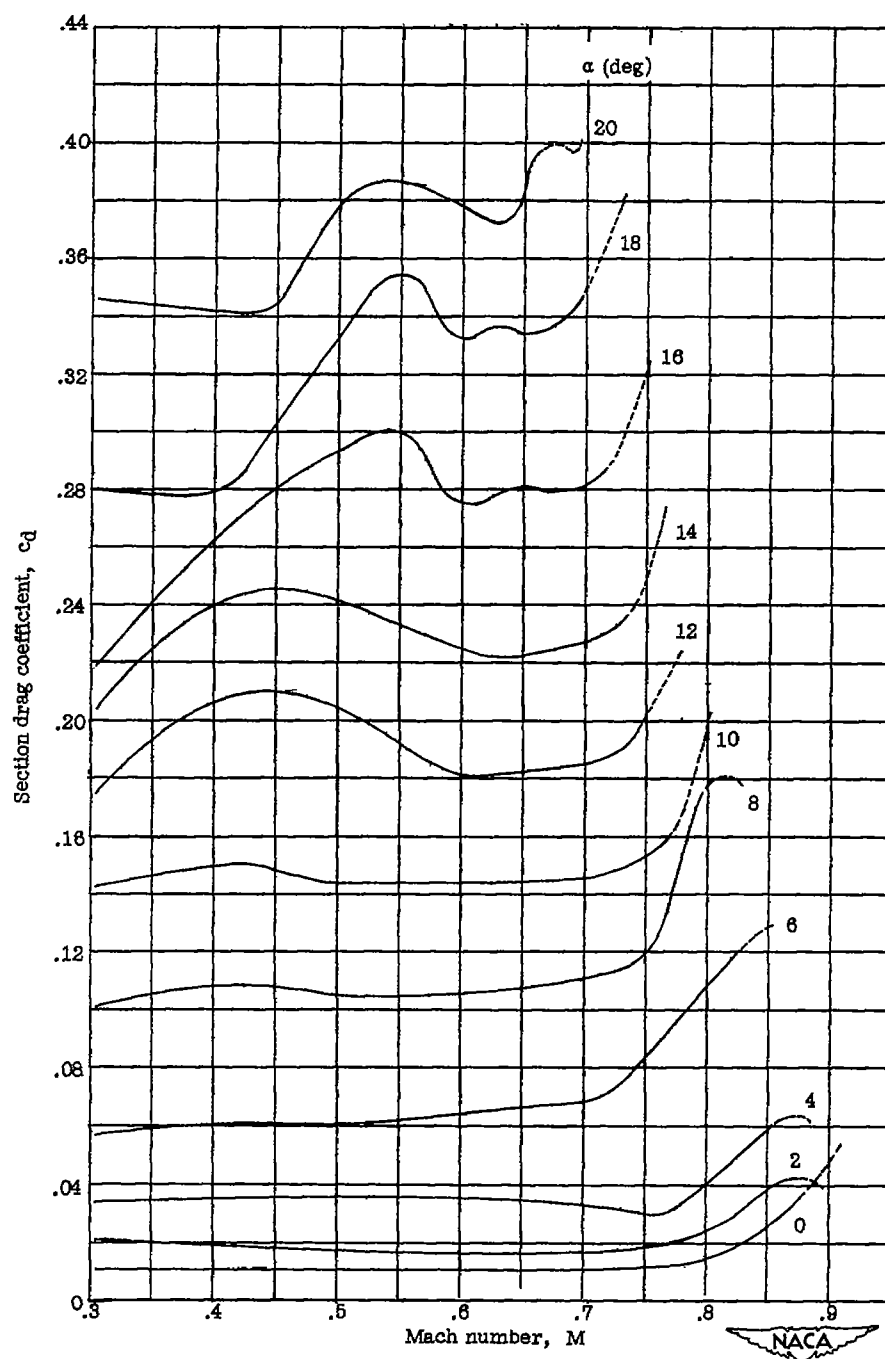
(g) W-3 airfoil.

Figure 7.— Continued.
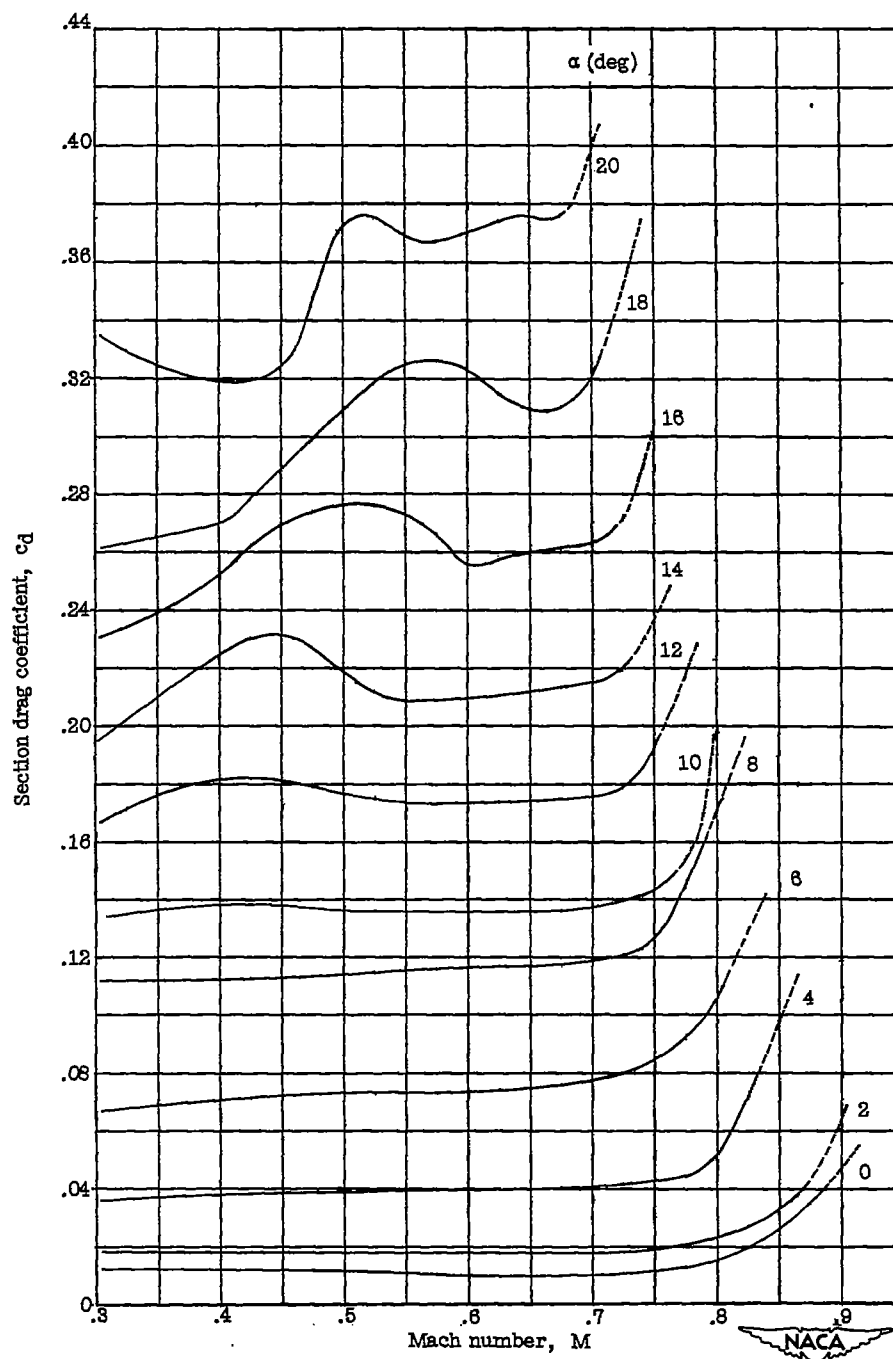
(h) W-7 airfoil.
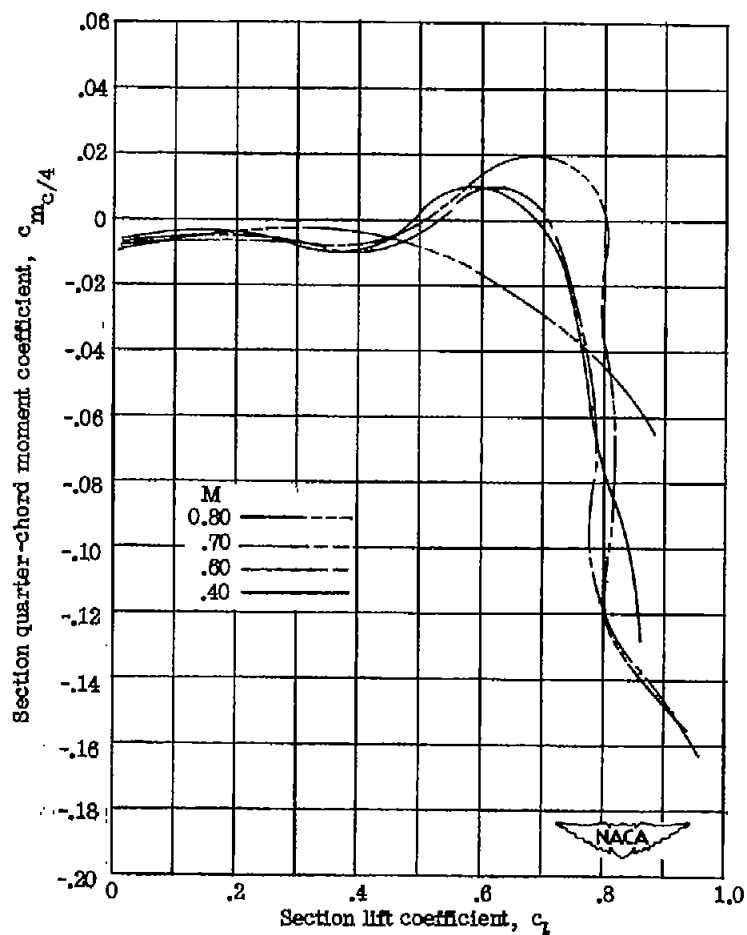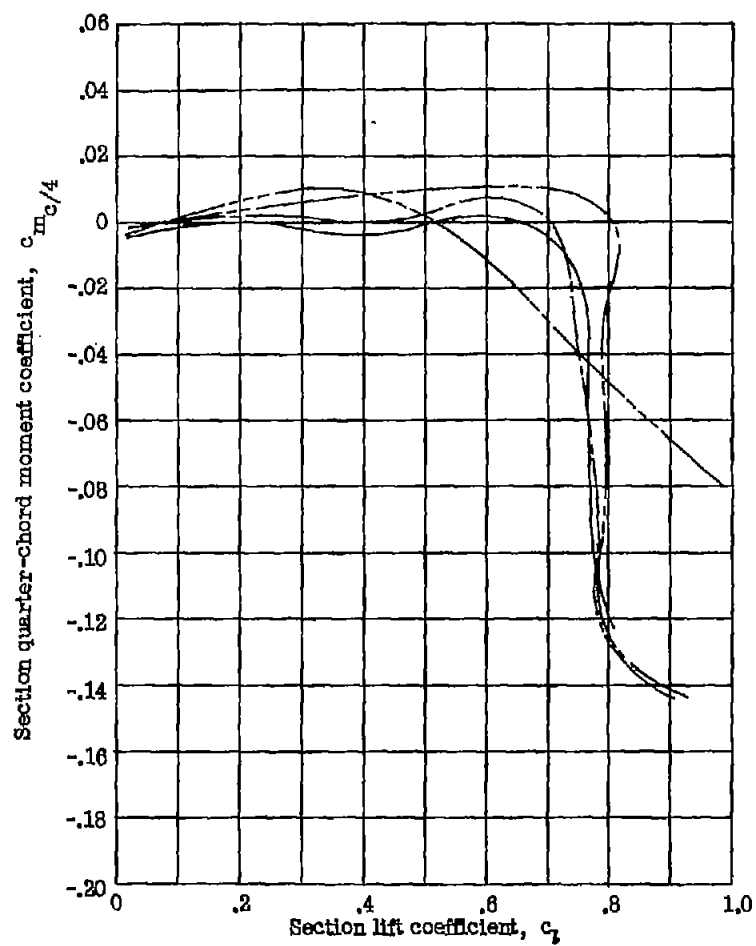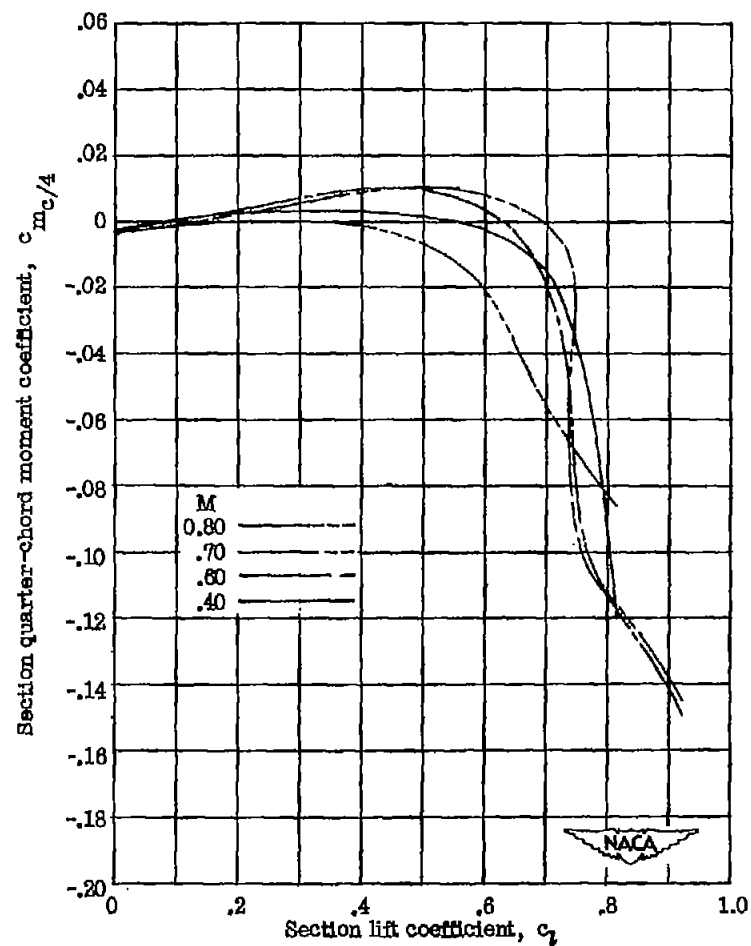
Figure 7.— Concluded.

(a)   NACA 16-006 airfoil.

(b)   NACA 66-006 airfoil.
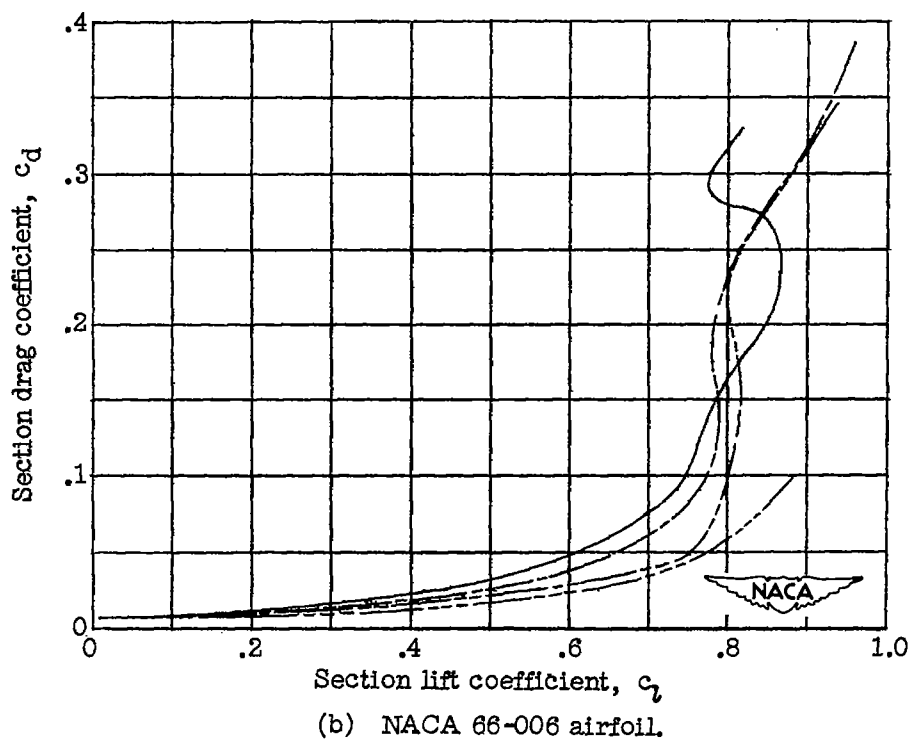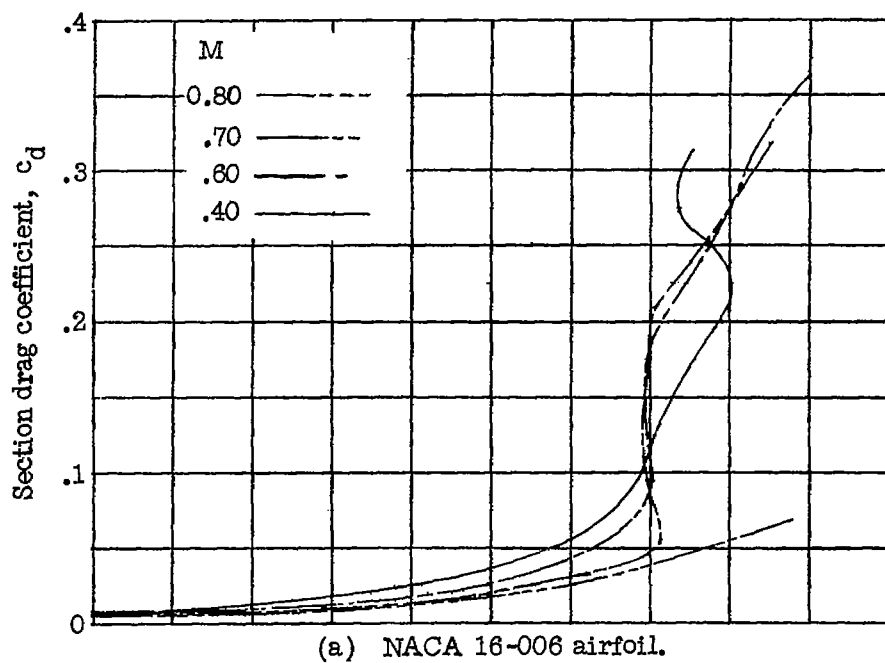
Figure 8.— Section-drag-coefficient variation with section lift
coefficient.

(c)   NACA 0006-63 airfoil.
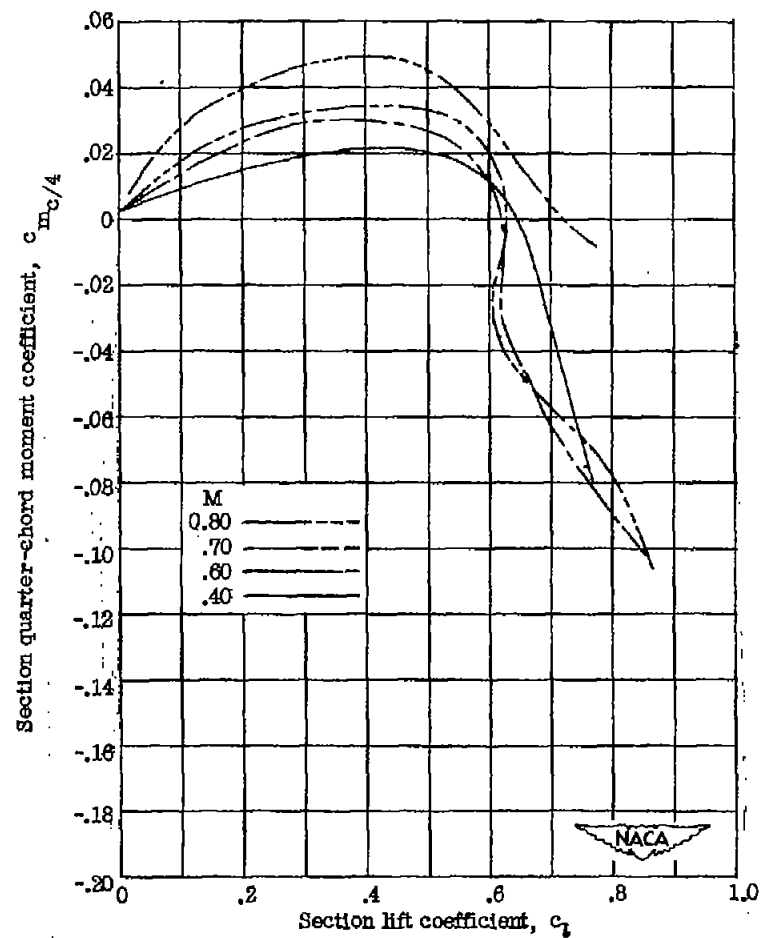
(d)   C-3 airfoil.

Figure 8.— Continued.

(e) C-5 airfoil.

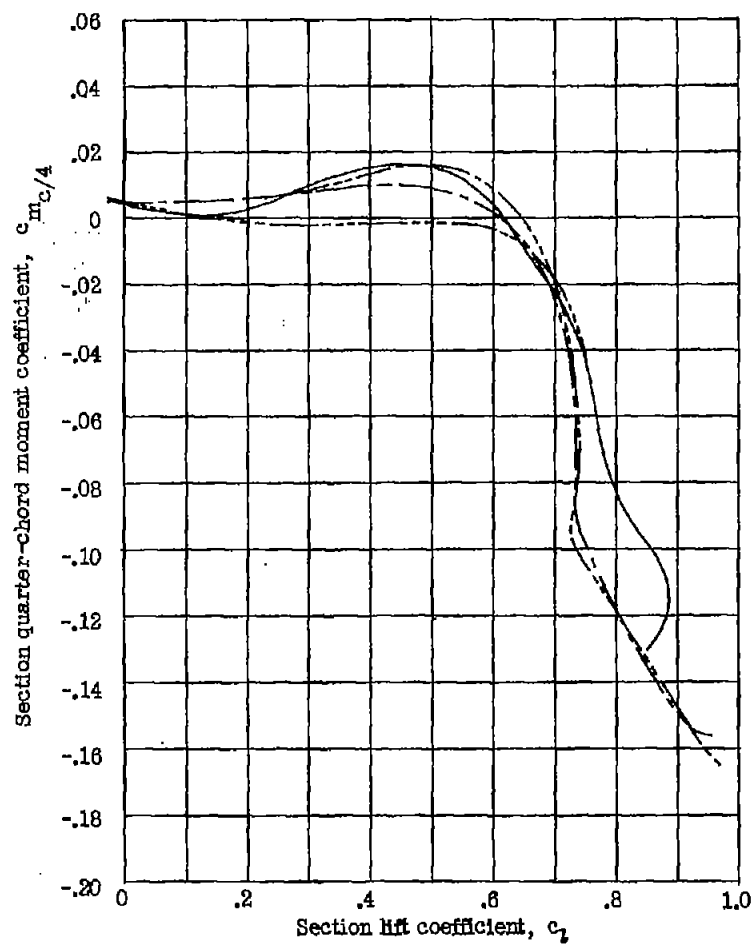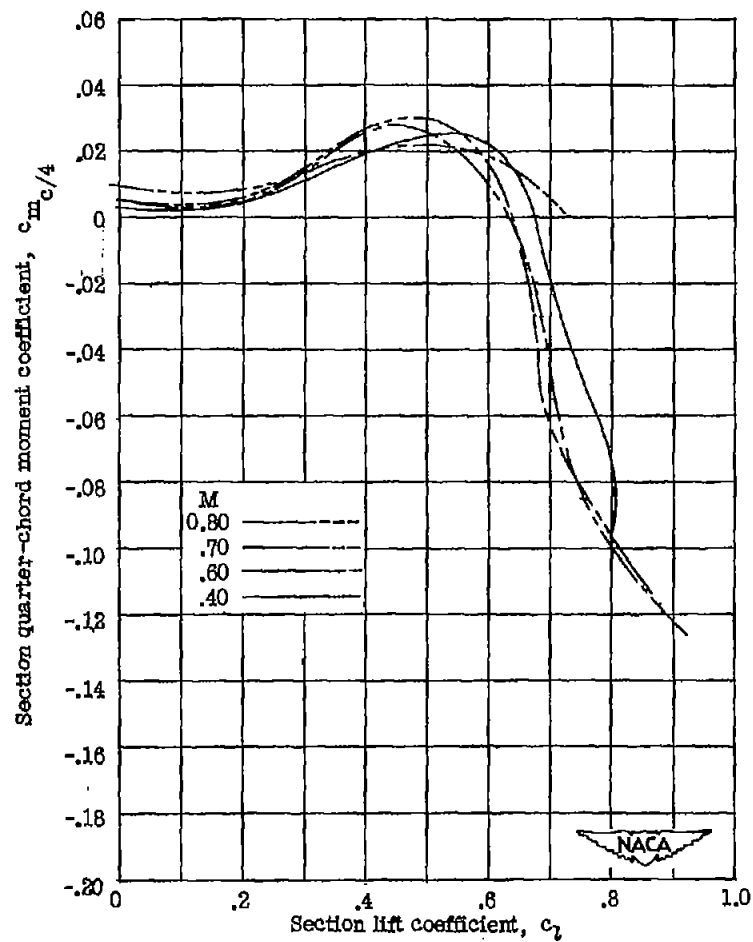(f) C-7 airfoil.

Figure 8.— Continued.

(g) W-3 airfoil.

(h) W-7 airfoil.
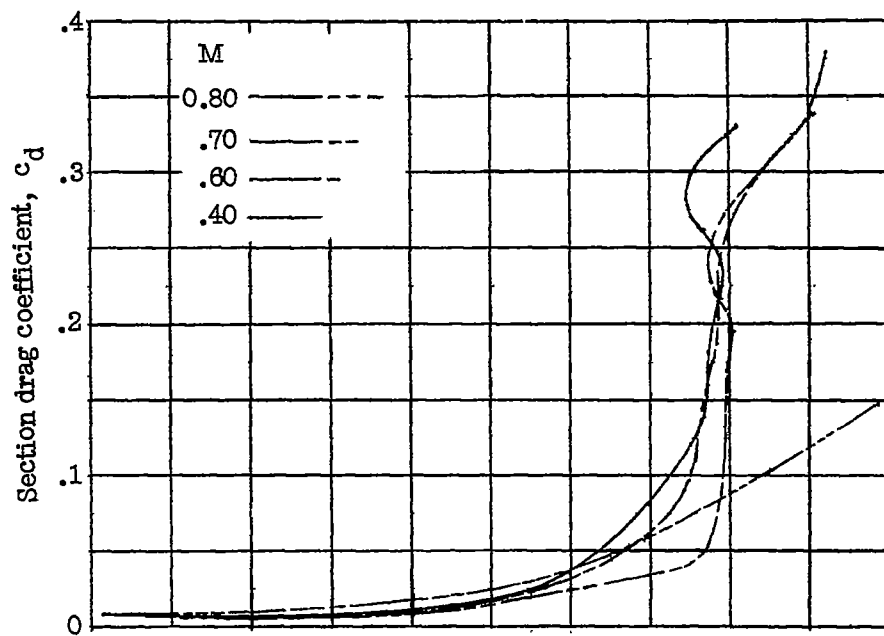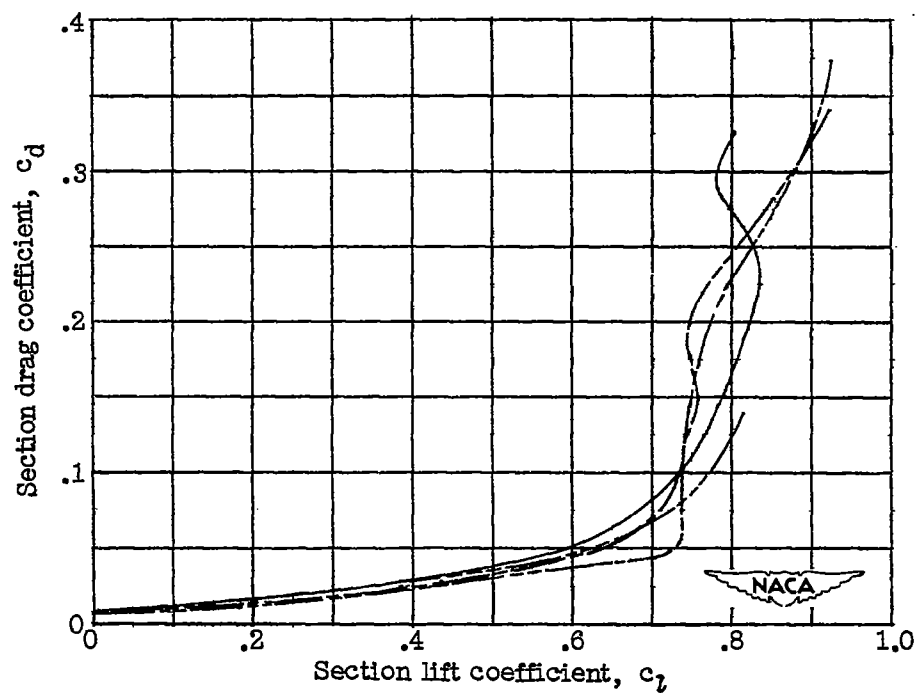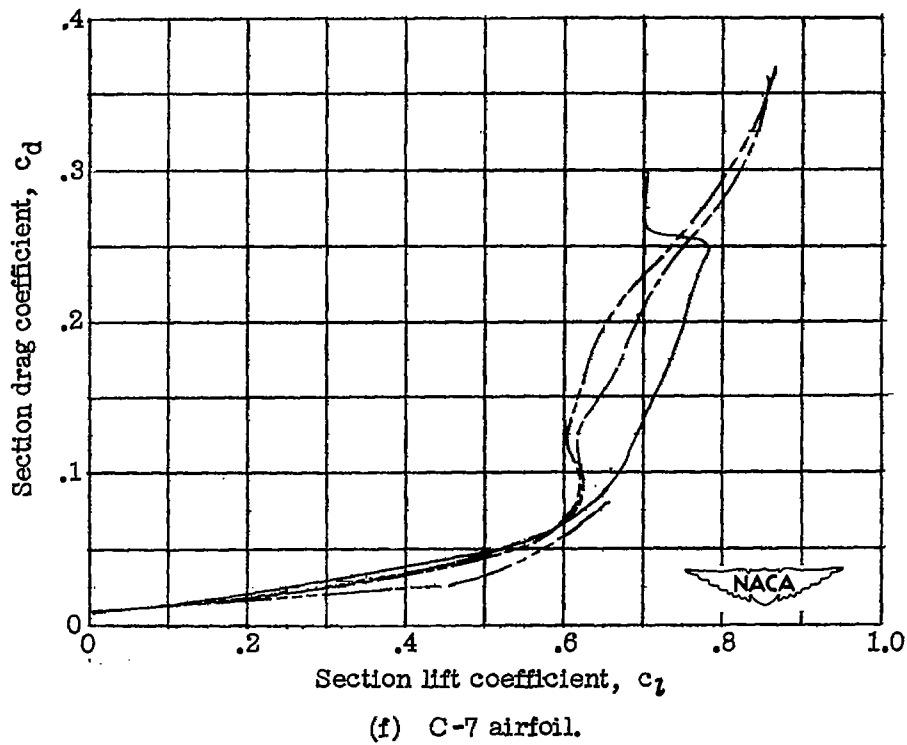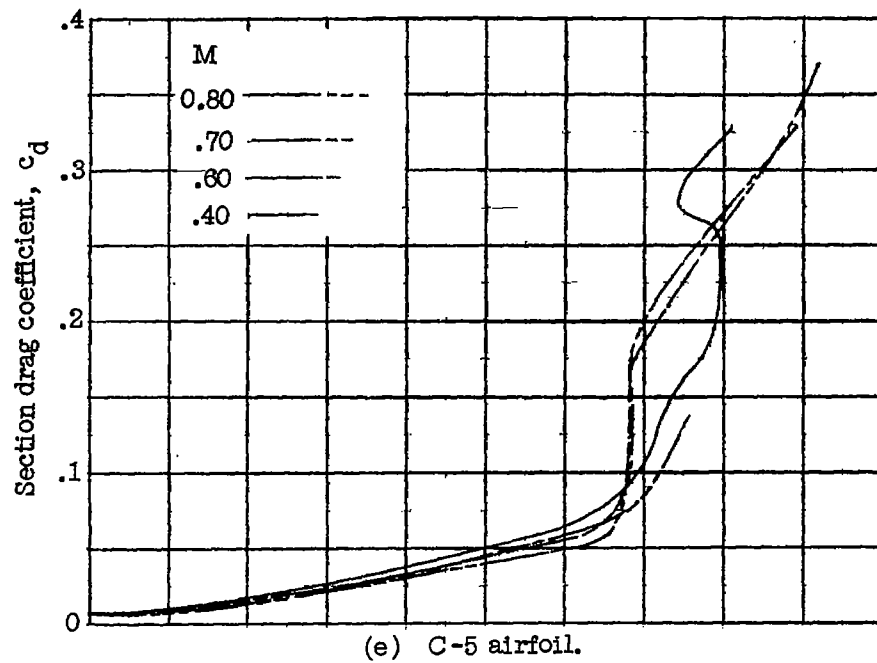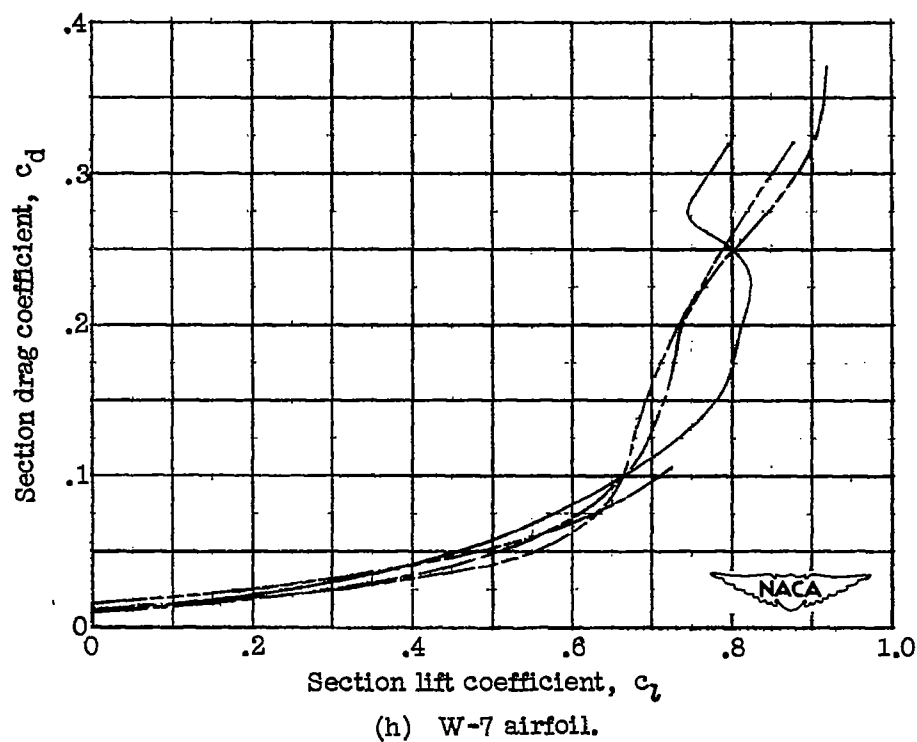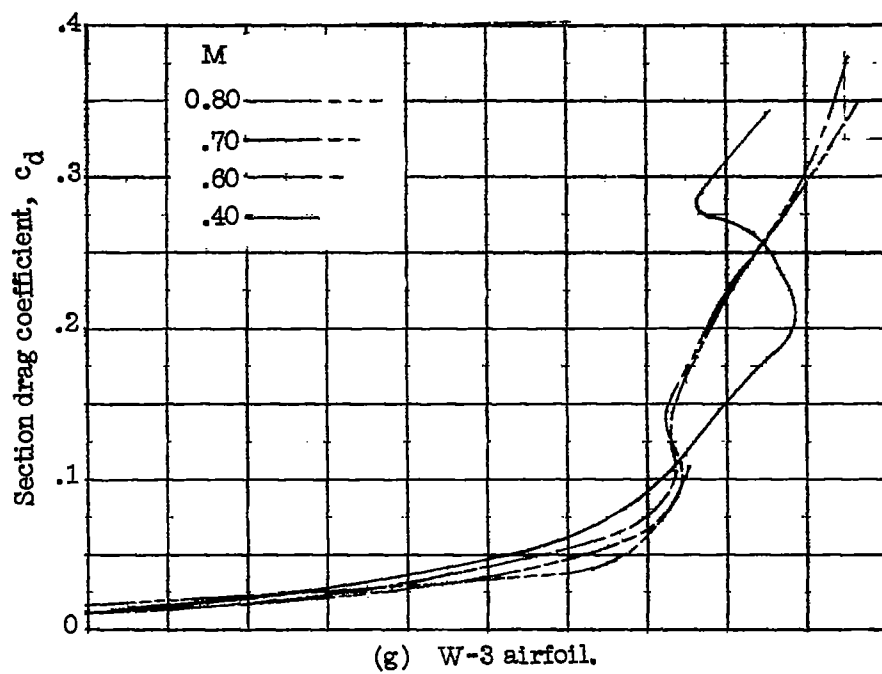
Figure 8.— Concluded.
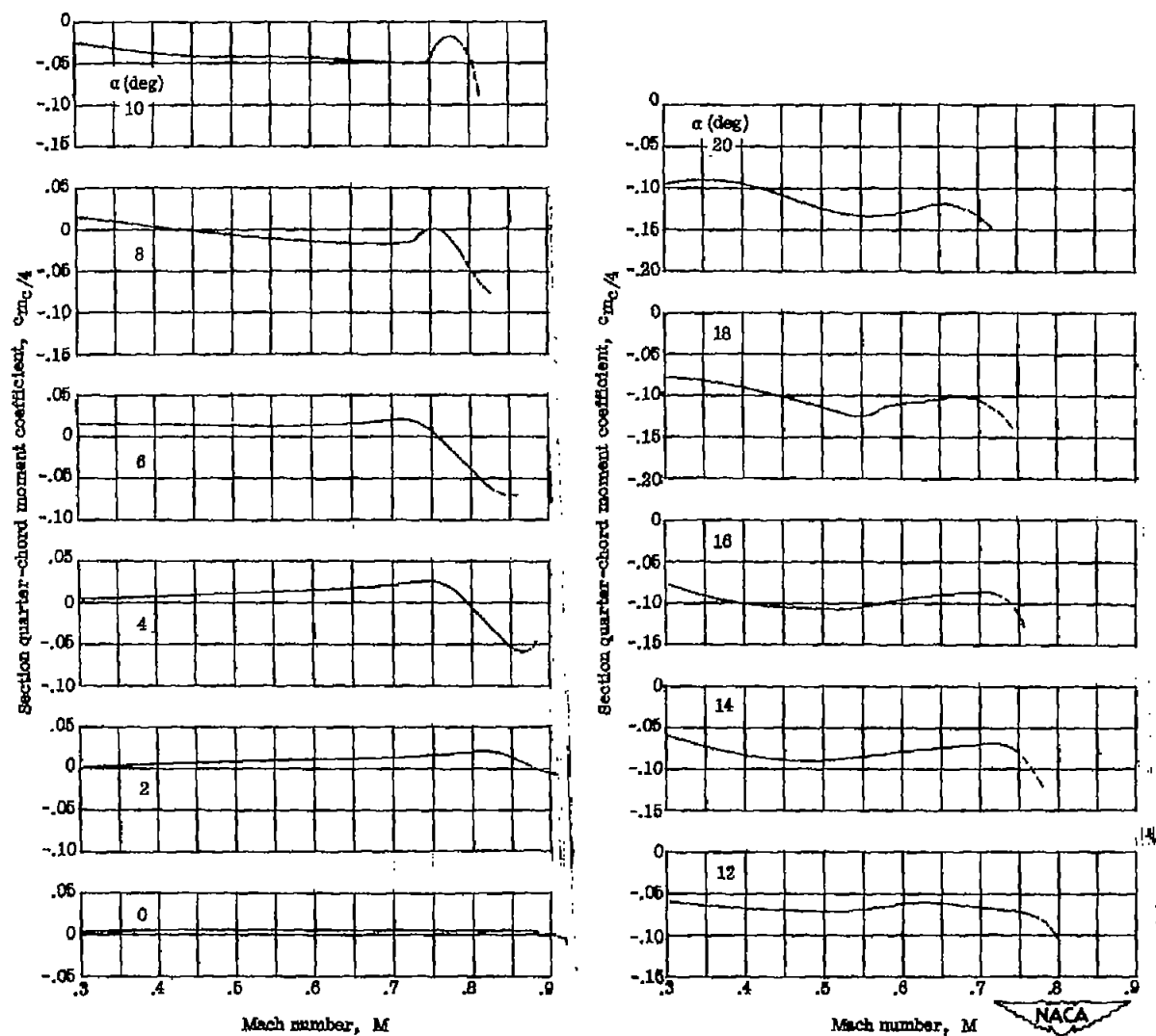
(a) NACA 16-006 airfoil.

Figure 9.- Variation of section pitching-moment coefficient about quarter-chord location $c_{m_c/4}$ with Mach number M. (Curves are dashed for data from $(M_{ch} - 0.030)$ to $M_{ch.})$
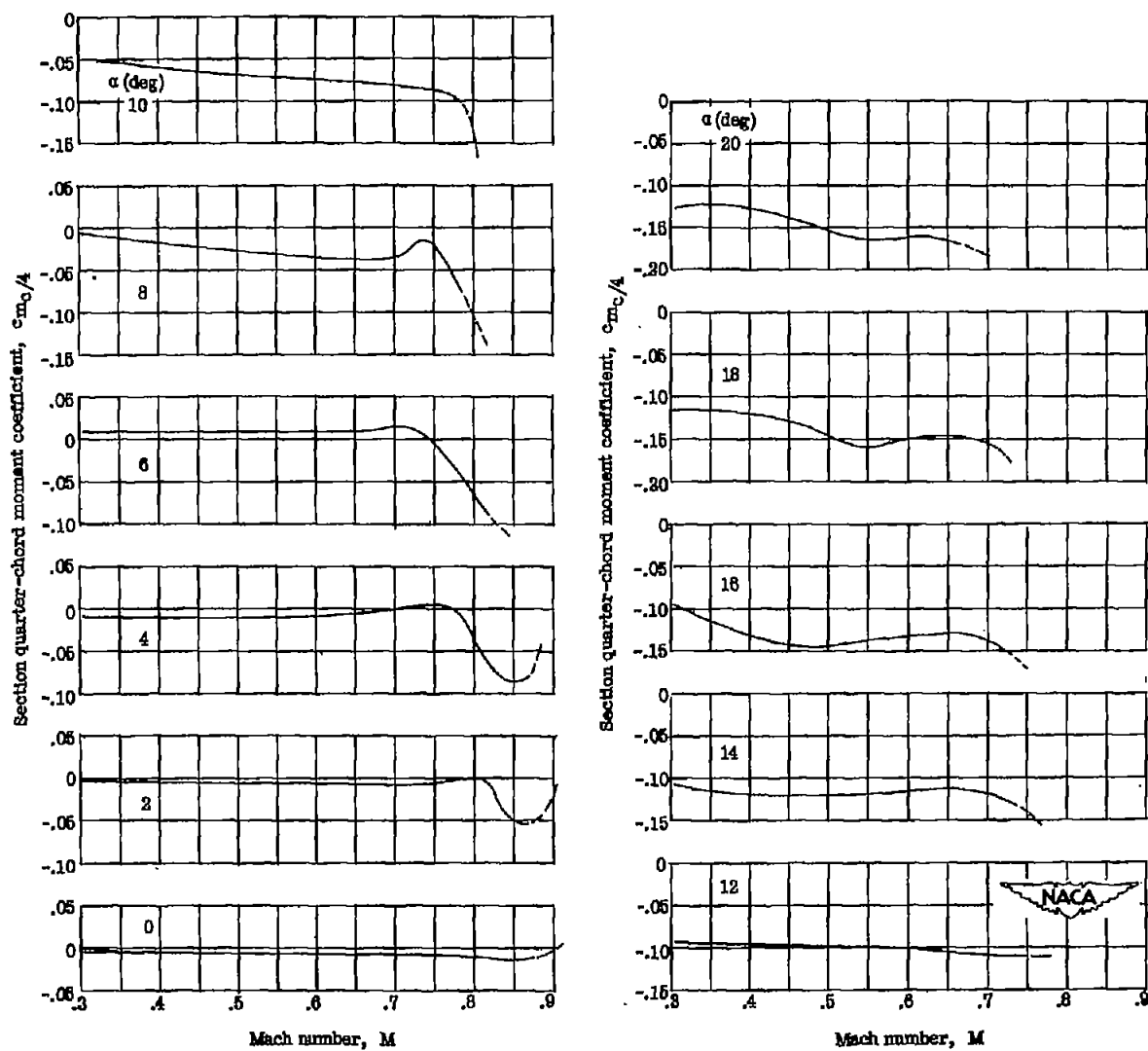
(b) NACA 66-006 airfoil.

Figure 9.– Continued.
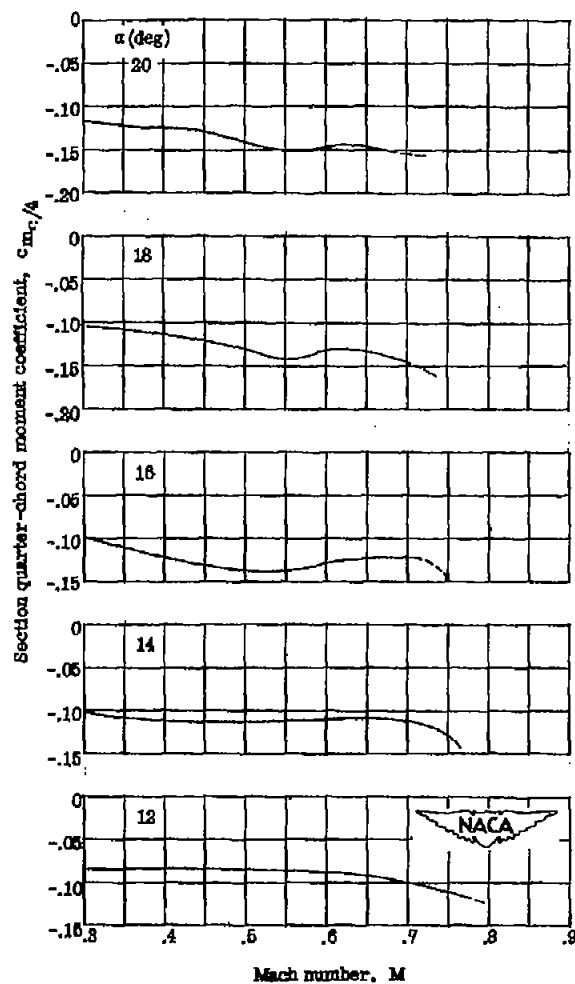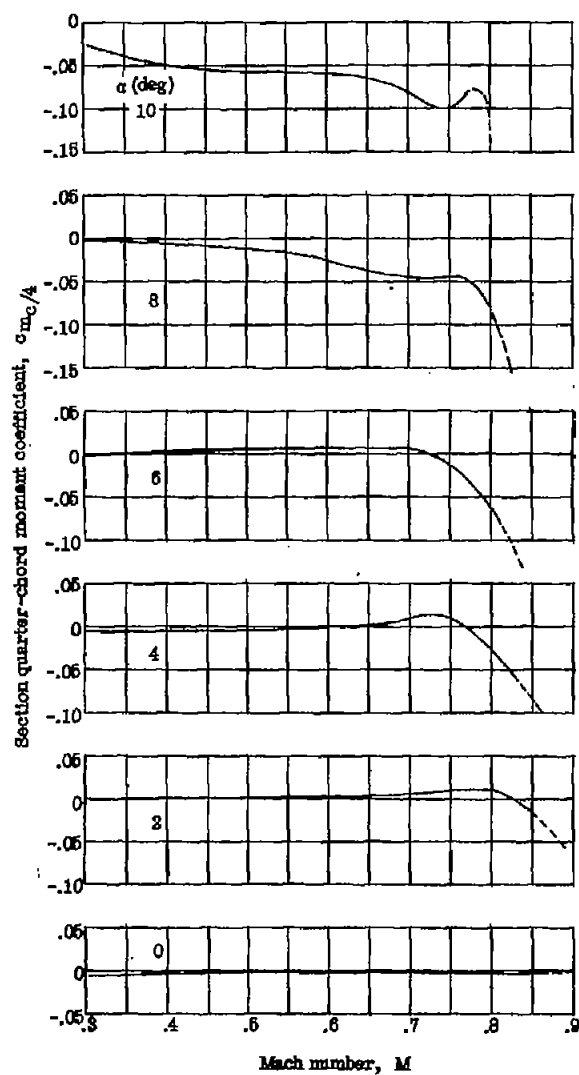
(c) NACA 0006-63 airfoil.

Figure 9.— Continued.

(d) C—3 airfoil.

Figure 9.— Continued.

(e)   C-5 airfoil.

Figure 9.— Continued.

(f) C-7 airfoil.

Figure 9.— Continued.

(g) W-3 airfoil.

Figure 9.- Continued.

(h) W-7 airfoil.

Figure 9.— Concluded.

(a) NACA 16-006 airfoil.

(b) NACA 66-006 airfoil.

Figure 10.— Variation of section pitching-moment coefficient about quarter-chord location with section lift coefficient.

(c) NACA 0006-63 airfoil.

(d) C-3 airfoil.

Figure 10.- Continued.
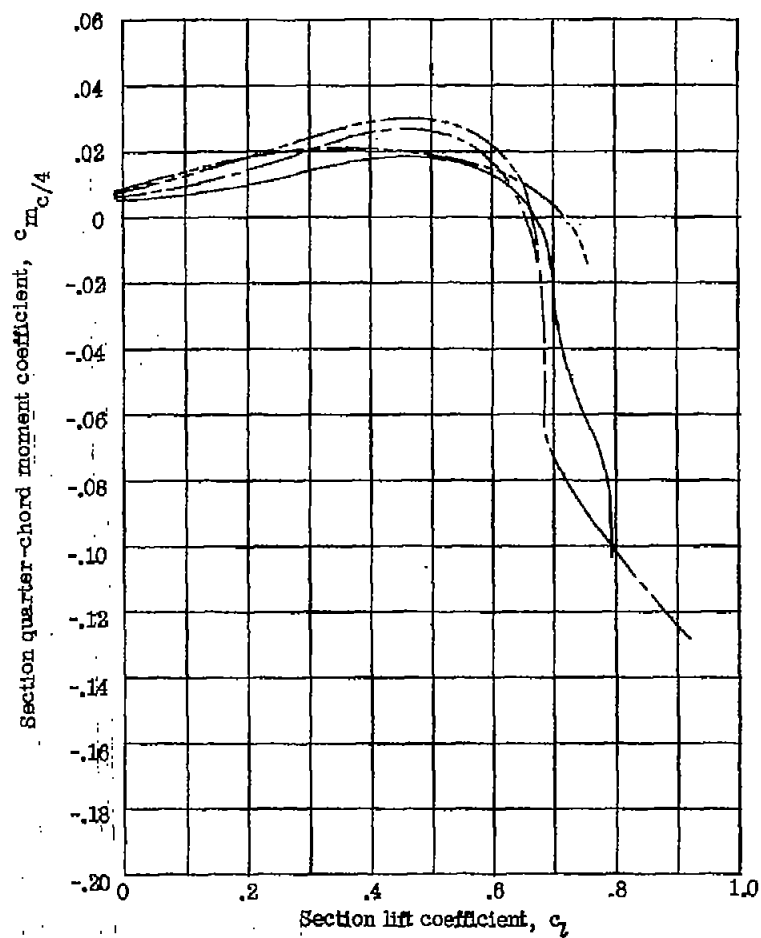
(e) C-5 airfoil.

(f) C-7 airfoil.

Figure 10.— Continued.

(g) W–3 airfoil.

(h) W–7 airfoil.

Figure 10.– Concluded.

Upper surface
Lower surface

M = 0.31

Pressure coefficient, P

M = 0.76

M = 0.84

NACA 0006-63 airfoil   C-3 airfoil   W-3 airfoil

Percent chord
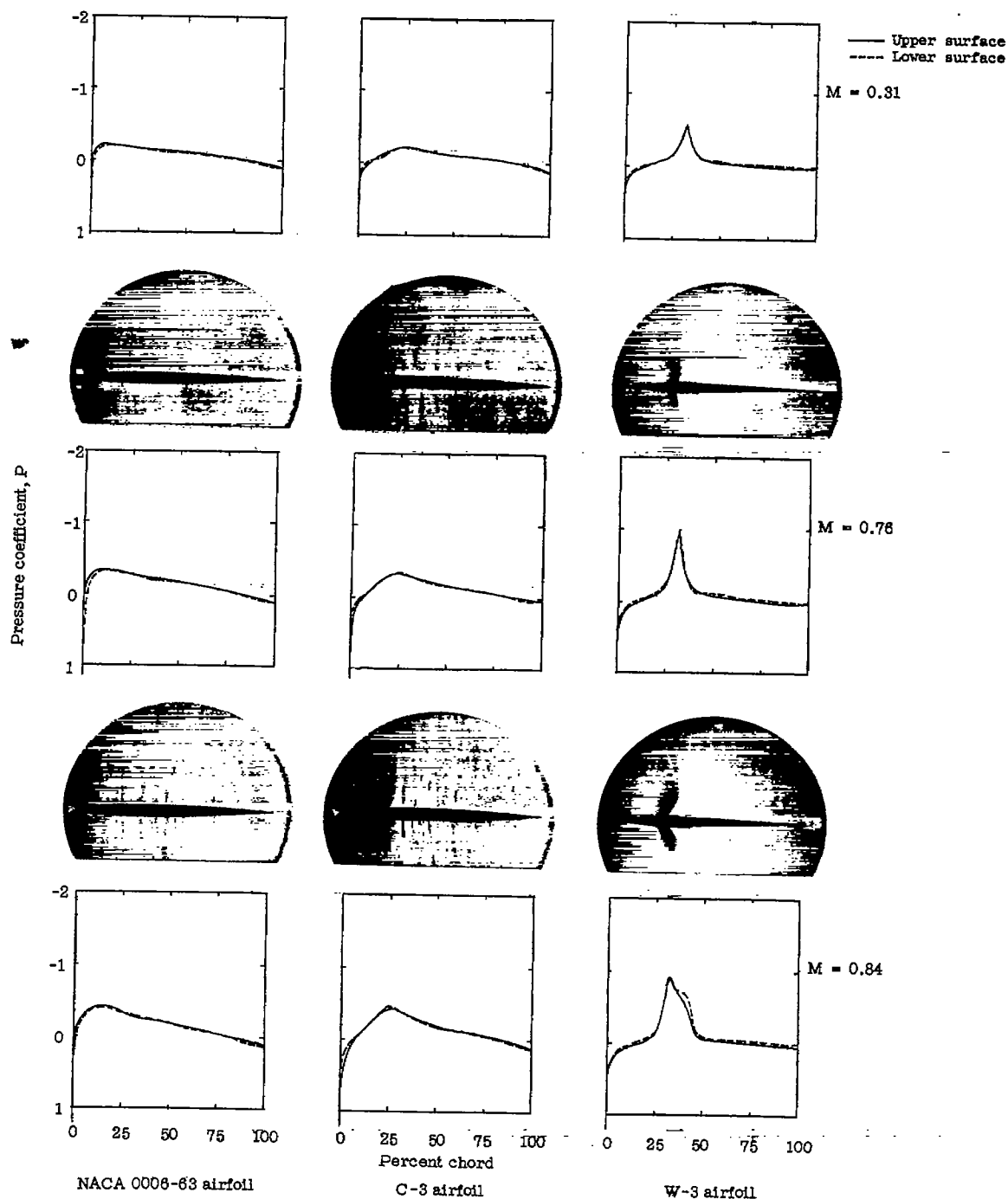
(a) α = 0°.

L-60563

Figure 11.— Representative schlieren photographs and pressure—distribution diagrams.

(b) α = 4°.

Figure 11.— Continued.

M = 0.31

M = 0.72
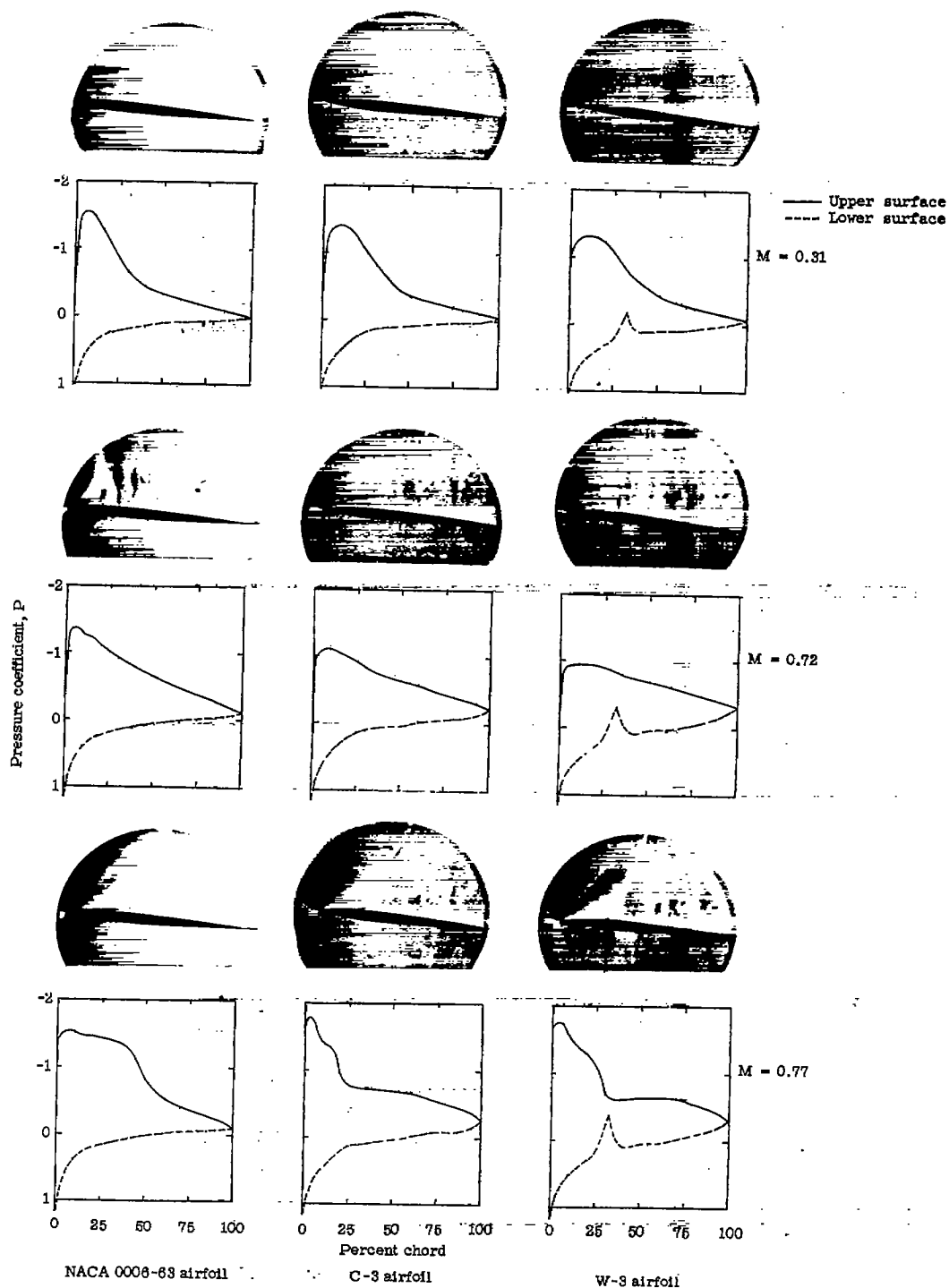
M = 0.77

Upper surface
Lower surface

Pressure coefficient, P

Percent chord

NACA 0006-63 airfoil   C-3 airfoil   W-3 airfoil
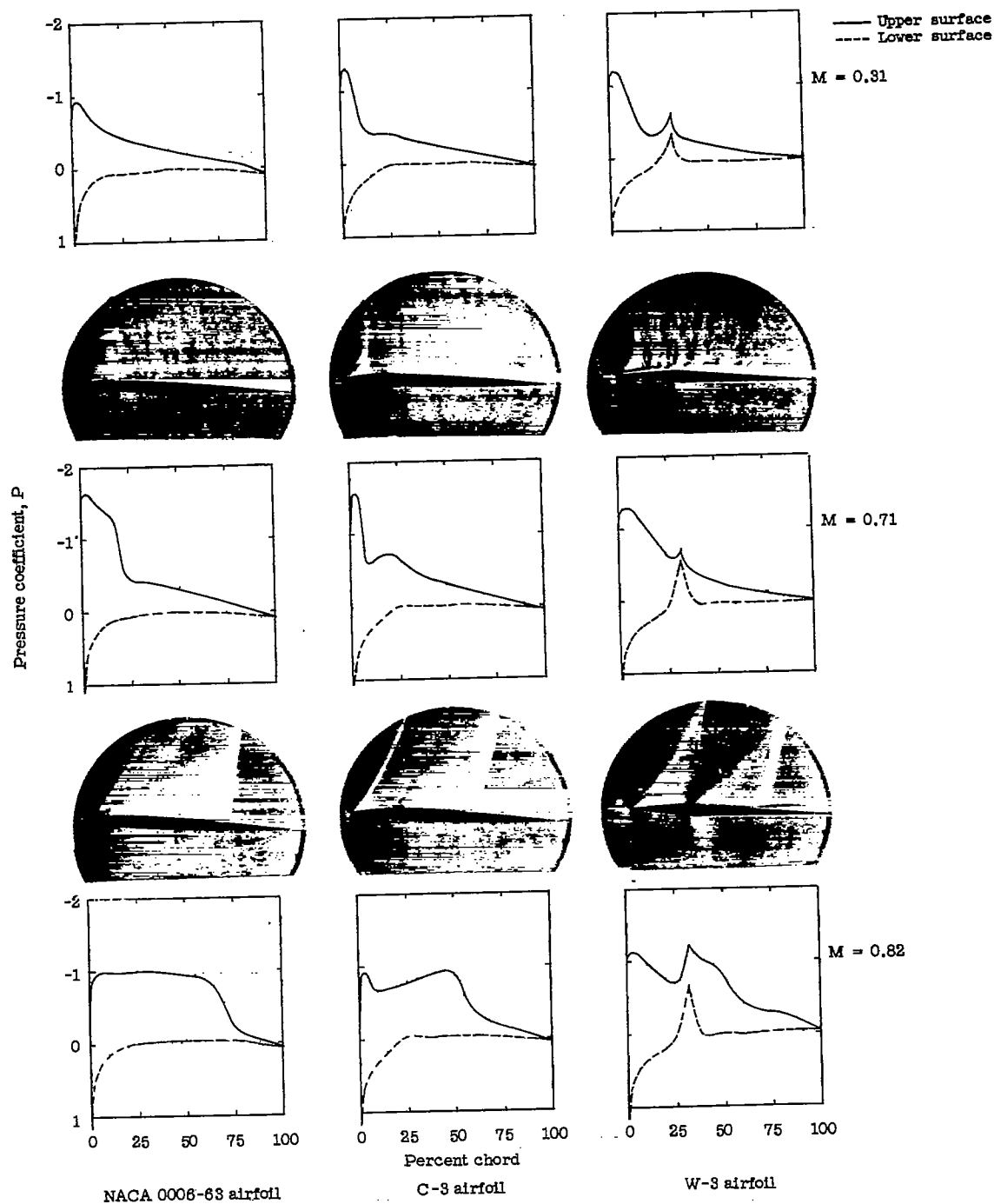
(c)   α = 8°.

L-60565

Figure 11.— Continued.
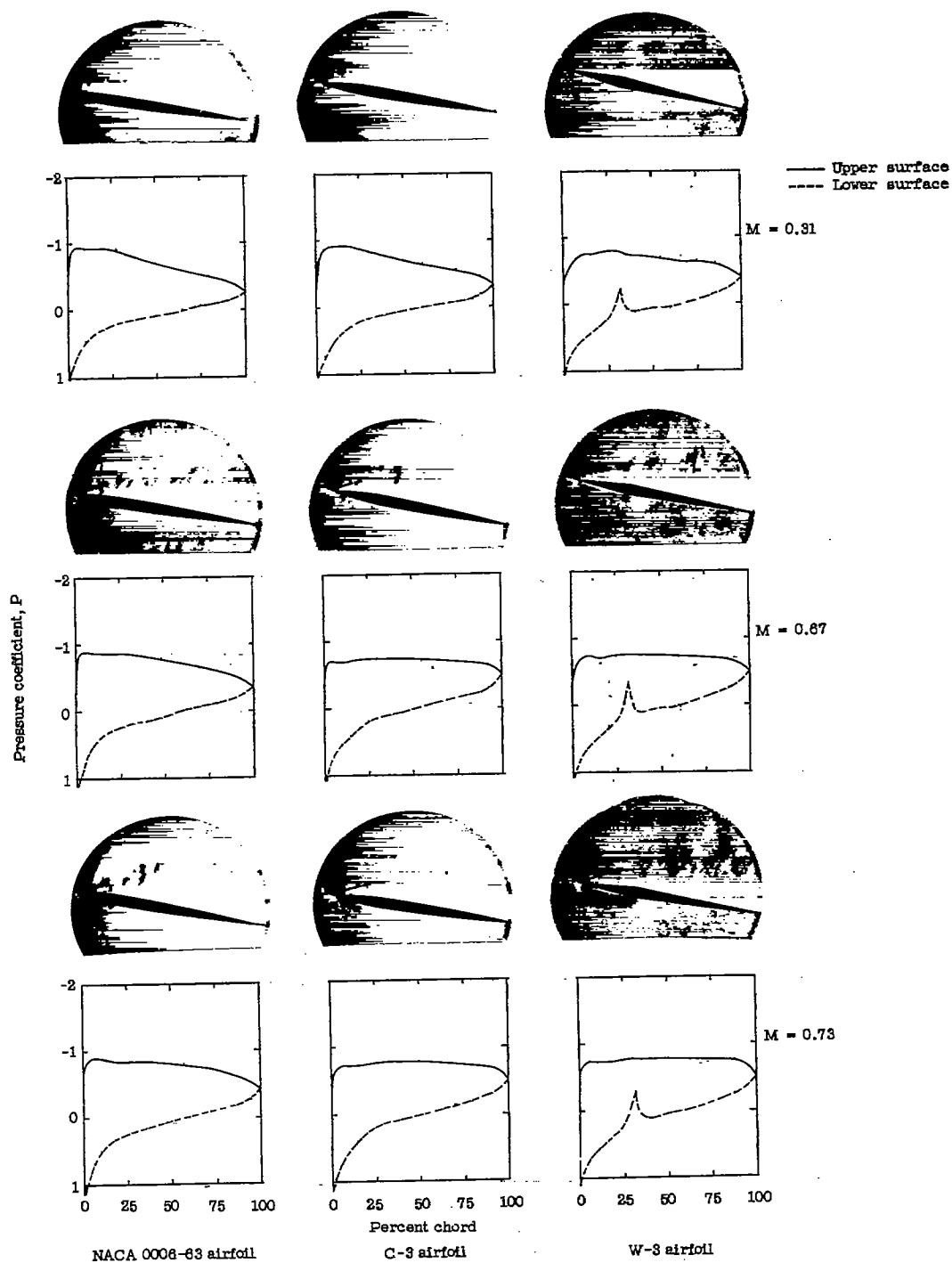
(d)   α = 12°.

L-60566

Figure 11.— Continued.

Upper surface
Lower surface

M = 0.31

M = 0.62

M = 0.71

Pressure coefficient, P

0   25   50   75   100
0   25   50   75   100
Percent chord
0   25   50   75   100

NACA 0006-63 airfoil

C-3 airfoil

W-3 airfoil

(e) $\alpha = 16^\circ$.
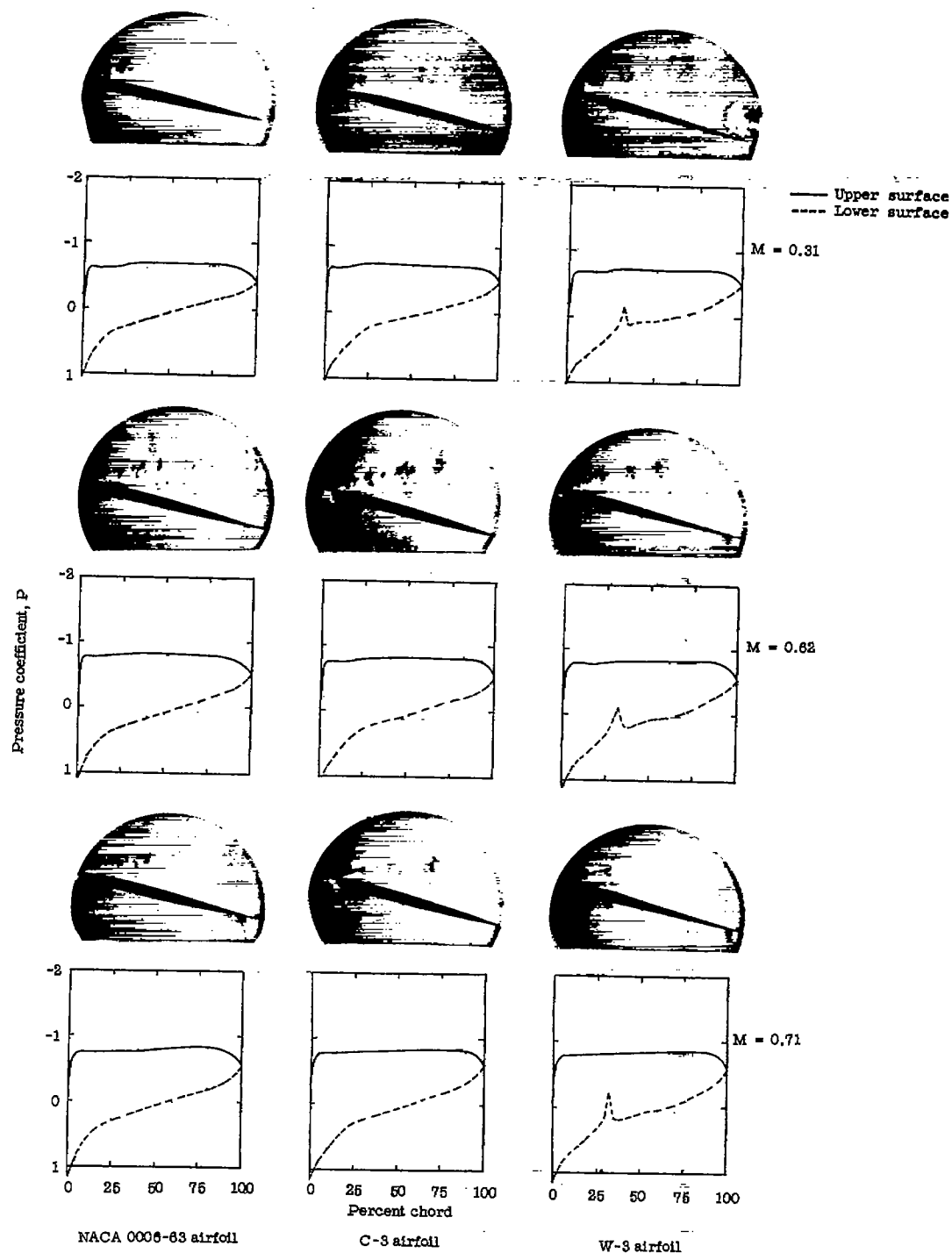
L-60567

Figure 11.— Continued.

(f)   α = 20°.
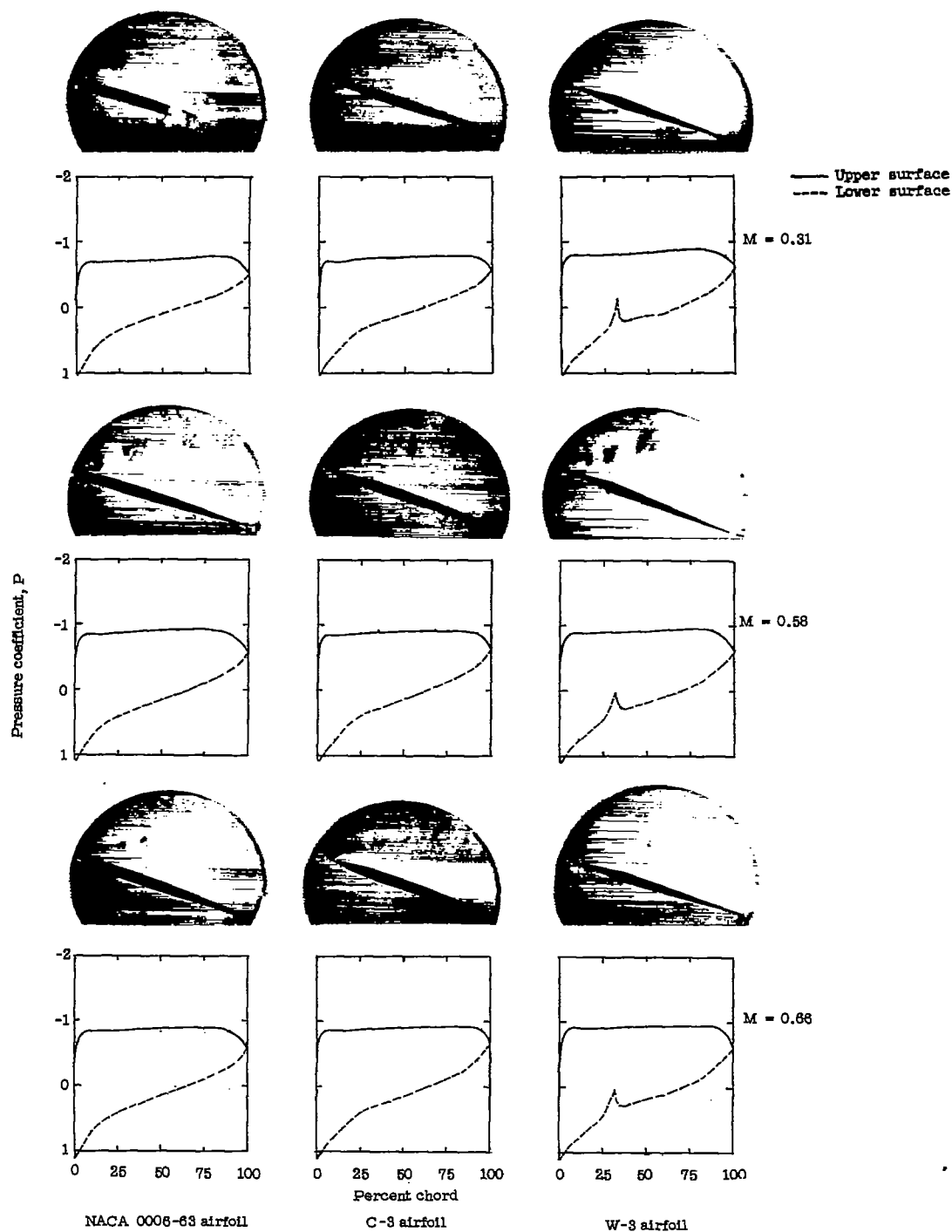
L-60568

Figure 11.— Concluded.